

University of Richmond

## UR Scholarship Repository

---

Honors Theses

Student Research

---

2015

### A computational investigation of halogen bonding with halomethanes and their group 14 analogues

William Kretz  
*University of Richmond*

Follow this and additional works at: <https://scholarship.richmond.edu/honors-theses>

 Part of the [Chemistry Commons](#)

---

#### Recommended Citation

Kretz, William, "A computational investigation of halogen bonding with halomethanes and their group 14 analogues" (2015). *Honors Theses*. 864.

<https://scholarship.richmond.edu/honors-theses/864>

This Thesis is brought to you for free and open access by the Student Research at UR Scholarship Repository. It has been accepted for inclusion in Honors Theses by an authorized administrator of UR Scholarship Repository. For more information, please contact [scholarshipprepository@richmond.edu](mailto:scholarshipprepository@richmond.edu).

A Computational Investigation of Halogen Bonding  
with Halomethanes and Their Group 14 Analogues

by

William Kretz

Honors Thesis

Submitted to

Department of Chemistry

University of Richmond

Richmond, VA

April 24, 2015

Advisor: Dr. Kelling Donald

This thesis by William Kretz has been approved by the following:



---

Advisor: Kelling J. Donald



---

Reader: René P. F. Kanters

**ABSTRACT:** It is known that halogen bonding is supported by so-called sigma holes on halides that interact with bases, but what are the limits of that interaction? How does the interaction depend on the group to which the halogen atom is bonded? To answer these questions, complexes of the form  $MH_3X\cdots Y$  (where  $M=C, Si, Ge, Sn, Pb$ ;  $X= F, Cl, Br, I$  and  $Y$  are Lewis bases) were optimized and their energetics and relative stability were assessed. The Lewis bases range from  $NH_3$  to the more complicated pentafluoropyridine (F-py). Calculations were performed entirely at the MP2(full) level of theory, including frequency analyses for the complexes. Additionally, their electrostatic potentials and interaction energies were used to determine the stability (or presence) of a halogen bond. Moderately strong halogen bonds are formed by some of these complexes, but quite weak halogen bonds and alternative interactions – evidently more favorable than halogen bonding - have been observed.

## 1. Introduction

Halogen bonding is a phenomenon long in existence in nature before it was named. As Legon notes<sup>1</sup>, the kinds of interactions that came to be called halogen bonding were observed as early as 1863, when Gunthrie<sup>2</sup> studied the complex  $I_2 \cdots H_3N$ . In that study, the interaction between the dihalogen with a Lewis base was observed. Although not labeled or thought of as halogen bonding at that time, other dihalide and Lewis base complexes continued to be observed experimentally<sup>3,4,5</sup> and studied further until chemists decided to pursue comprehensive theoretical studies into interactions of this form<sup>6,7</sup>, which eventually became known as halogen bonding.

Today a halogen bond is considered a complex of the form  $Y \cdots X-R$ , where Y: is an electron rich Lewis base and X is a halogen substituent on an XR molecule or ion.<sup>8</sup> Because of the nature of this interaction, Legon goes as far as to call the halogen bond an analogue of a hydrogen bond.<sup>1</sup> The peculiarity of these interactions comes from the fact that the interactions occur with a  $180^\circ$  angle between formed by the  $Y-X$  and  $X-R$  bonds, and that orientation has come to be an indicator that there is a stable interaction between Y and the halogen X.<sup>8</sup>

It has been found that the  $X \cdots Y$  interaction is favored by the presence of a so-called a sigma hole on X.<sup>9</sup> This hole is an area of positive potential that develops on an atom in a molecule that is bonded to moderately to strongly electron-withdrawing atoms - in this case R to which X is bonded.<sup>9</sup> Below in Figure 1, the potential surfaces generated by Clark<sup>9</sup> of  $CF_4$ ,  $CF_3Cl$ ,  $CF_3Br$ , and  $CF_3I$  are shown

demonstrating how the sigma hole grows as a F atom on  $\text{CF}_4$  is replaced by Cl, Br, and I.

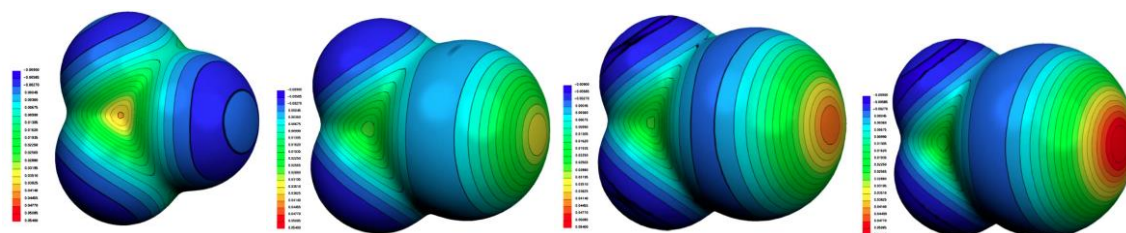


**Figure 1:** Sigma Holes for  $\text{CF}_4$ ,  $\text{CF}_3\text{Cl}$ ,  $\text{CF}_3\text{Br}$  and  $\text{CF}_3\text{I}$ : These potential surfaces were generated by Clark<sup>9</sup>. Starting from the left, they are the molecules  $\text{CF}_4$ ,  $\text{CF}_3\text{Cl}$ ,  $\text{CF}_3\text{Br}$  and  $\text{CF}_3\text{I}$ . Areas of blue are the most negative, while areas of red are the most positive.

These regions of positive potentials (called 'holes' even though they are not empty spaces, but just regions of net positive potentials), allow for attractive interactions with electron rich atoms or molecules, like Y in this case. Clark notes that the size and presence of these holes depends on various factors, including the electron withdrawing power of R.<sup>9</sup> In the case of  $\text{CF}_3\text{X}$  shown above (where  $\text{R} = \text{CF}_3$ ), the holes generated rely on the three fluorine atoms pulling electron density from C and consequently from X to create the hole.

The importance of the sigma hole in halogen bonding has caused Donald et al.<sup>10</sup> to address how the atoms of the XR molecule affect the size and strength of the molecule's sigma hole. In their investigation, ternary  $\text{MX}'_{4-n}\text{X}_n$  molecules ( $\text{M} = \text{C}, \text{Si}, \text{Ge}, \text{Sn}, \text{Pb}$ ;  $\text{X} = \text{F}, \text{Cl}, \text{Br}, \text{I}$ ;  $\text{X}' = \text{H}, \text{I}, \text{F}$ ) were studied computationally to determine how the sigma hole changed as different atoms were used for the center and its substituents. The tested molecules were forced to interact in a  $180^\circ$  with  $\text{NH}_3$  in order to determine the interaction energies of the halogen bonds that formed. They found that the largest sigma holes and the most stable interactions formed when I

was used as the halogen (X) and three F atoms were used as the substituents on the center atom (X'). Additionally, they noticed a trend that the sigma hole increased in strength as the halogen was changed going down the periodic table from F to I, but it decreased when the center atom was changed down the periodic table from C to Pb.<sup>10</sup>

Even with the sigma hole's presence, a halogen bond still requires another molecule to complex with. Using the notion mentioned previously, the Y molecule, acting as a Lewis base, in the YXR complex can also influence the development of a sigma hole and the stability of a halogen bond interaction since it provides the negative potential to interact with the positive potential of the sigma hole. Donald's work with halogen bonding continued to address this with a computational investigation done in collaboration with Tawfik<sup>11</sup> that focused on how the Lewis base affects the development of a halogen bond. They made a number of significant observations on the nature of halogen bonding R-X species of the form MF<sub>3</sub>X (R = C, Si, Ge, Sn, Pb; X = F, Cl, Br, I) in complexes with various Lewis bases. Their results showed that halogen bonding was possible with many of the molecule combinations they tried, but they were limited to highly fluorinated systems.

In order to provide a more complete picture of halogen bonding, a similar approach that Tawfik and Donald<sup>11</sup> took was taken in this work, but with RX species of the form MH<sub>3</sub>X. Thus, this study looked into whether halogen bonding occurred even when the electron-withdrawing power was significantly lower than in the case where R=CF<sub>3</sub>. With this information, our current understanding of halogen bonding could be expanded to create a more unifying perspective on the phenomenon.

The hope was that the theoretical work done here and in the future could help aid researchers who have observed these interactions experimentally.<sup>12</sup> Currently, very little is known about these interactions when compared to other well-studied topics in chemistry. They have been observed in important fields of research such as drug design<sup>13</sup>, biology<sup>14</sup>, and crystal engineering<sup>15</sup>, which further raises the need to study halogen bonding. Knowing the conditions and environments under which sigma holes form and halogen bonding occurs would allow experimentalists to utilize the interactions to better understand larger concepts in their fields.

As was done by Tawfik and Donald<sup>11</sup>, 104 combinations of molecules were considered as possibly being able to halogen bond. The molecules, listed in Table 1, include three halomethanes and the Si, Ge, Sn, and Pb analogues of halomethane interacting with various Lewis bases. Some phosphorous centered Lewis bases were tested as well, but due to their lack of halogen bonding, they were omitted from the data shown in this work. The bases were picked because they are commonly used as reagents in the organic and inorganic chemistry. From these bases, some alterations were made to provide diversification of the bases (eg. NH<sub>3</sub> and NF<sub>3</sub>).

R-X (where R=H <sub>3</sub> M-)		Y		
CH <sub>3</sub> F	SnH <sub>3</sub> I	H <sub>2</sub> O	H <sub>2</sub> S	NF <sub>3</sub>
CH <sub>3</sub> Cl	GeH <sub>3</sub> I	CH <sub>3</sub> OCH <sub>3</sub>	SeH <sub>2</sub>	NCl <sub>3</sub>
CH <sub>3</sub> Br	SiH <sub>3</sub> I	THF	NH <sub>3</sub>	NBr <sub>3</sub>
CH <sub>3</sub> I	PbH <sub>3</sub> I	furan	N(CH <sub>3</sub> ) <sub>3</sub>	pyridine (Py)
				pentafluoropyridine (F-Py)

**Table 1:** List of Halomethanes and Heavier (R-X) Species and the Lewis Bases (Y) Considered in This Work: R-X refers to the Lewis acids tested in this study. Y refers to the Lewis bases.



## 2. Methods

Geometric visualization and manipulation of all the models of the complexes studied were done using ChemCraft and GaussView5 graphics software.<sup>16</sup> The same software was also used for generating electrostatic potential (ESP) representations. All calculations were done at the MP2(full) level of theory<sup>17</sup> and ab initio calculations were implemented using the Gaussian 09 (Rev. A.02, D.02) suite of programs.<sup>18</sup> The cc-pVTZ bases sets were utilized for the smaller atoms, while for the larger atoms (Pb, Sn, I), scalar-relativistic energy-consistent small core Dirac-Fock (MDF) effective-core pseudopotentials (ECPs) were used with 28 core electrons for Sn and I and 60 core electrons for Pb, along with the corresponding cc-pVTA-pp basis sets.<sup>19,20,21</sup> Basis-set superposition errors were corrected for using the counterpoise correction procedure.<sup>22</sup> These methods were chosen to be consistent with Tawfik and Donald's previous work<sup>11</sup> so that the two studies could be compared.

## 3. Results and Discussion

**3.1. Geometry and Stability.** The RX and Y species were optimized independently in each case and so were the complexes in order to find the energy minima. Because halogen bonding was the primary focus of this work, and because other geometrical configurations can also provide stability, it was necessary to initially orient the molecules so that the angle of RX-Y was as close to 180° as possible. This came from the literature<sup>8</sup>, where it has been found that halogen bonding generally occurs at an angle of 180°. With this initial geometric setup, the

complexes optimized to a halogen bond interaction if that arrangement was sufficiently favorable. After being optimized at the MP2(Full) level of theory, the complexes were analyzed to identify the presence of halogen bonding. The resulting optimized angles of interaction and interaction distances are given in Tables 2 and 3, respectively. It should be noted that based on the bond angles, it was possible to determine if a halogen bond did not form. As was previously stated, nearly linear angles are signs of halogen bonding since the sigma hole occurs directly opposite the R-X sigma bond.<sup>8</sup> Thus any bond angles not close to being linear were immediately suspected of not have formed a halogen bond. In cases where that suspicion was confirmed, the bond distances between the molecules are omitted from Table 3.

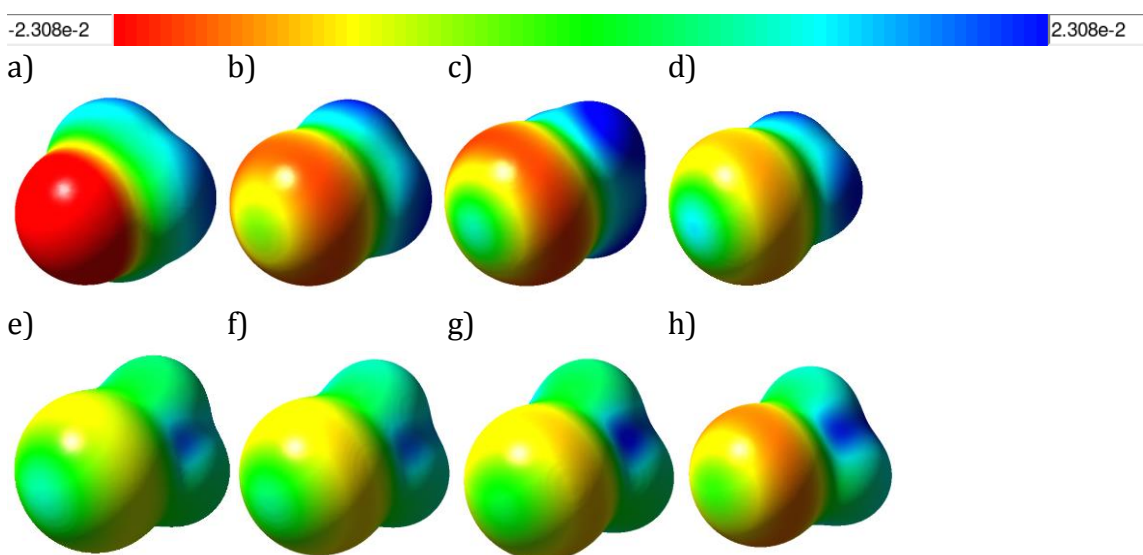


**Figure 2:** Sigma Holes On Lewis Acids: Computed ESP maps on the 0.02 iso-density surface for a)  $\text{CH}_3\text{F}$ , b)  $\text{CH}_3\text{Cl}$ , c)  $\text{CH}_3\text{Br}$ , d)  $\text{CH}_3\text{I}$ , e)  $\text{SiH}_3\text{I}$ , f)  $\text{GeH}_3\text{I}$ , g)  $\text{SnH}_3\text{I}$ , and h)  $\text{PbH}_3\text{I}$ . The ESPs on the surface shown are in the range  $\pm 2.308 \times 10^{-2}$  au. It should also be noted that unlike the previous figure (Figure 1) red denotes negative potential and blue denotes positive potential. This designation remains constant for the remainder of this work.

In this work, an angle of  $150^\circ$  was used to initially eliminate molecular pairs that did not have a halogen bond. This decision was supported strongly by the large gap between the sets of molecules with bond angles above and below  $150^\circ$  in Figure 3.

As can be seen in Table 2 and Figure 3, many of the molecules did not exhibit halogen bonding character based on their bond angle. This result varied greatly from Tawfik and Donald's previous work<sup>11</sup>, which found halogen bonding character with most of the complexes using  $\text{MF}_3\text{X}$  instead of  $\text{MH}_3\text{X}$ . While the results were different, the difference was expected. As was noted earlier, halogen bonding relies on electron withdrawing atoms to form the sigma hole on the  $\text{RX}$  complex. In Tawfik's work<sup>11</sup>, the  $\text{MF}_3\text{X}$  molecules had the electronegative F atoms to create the sigma hole. Thus, the size and strength of the sigma hole was larger for  $\text{MF}_3\text{X}$  than it was for  $\text{MH}_3\text{X}$ . The result, of course, was that the halogen bonding measured by Tawfik was stronger and more common among the complexes tested. In this work with  $\text{MH}_3\text{X}$ , the sigma holes were smaller and weaker due to the F atoms being replaced with H atoms, so the molecule relied more heavily on the Lewis base to stabilize an attraction with the sigma hole. One trend observed by Donald et al.<sup>10,11</sup> that remained even without the F atoms attached to  $\text{MH}_3\text{X}$  was that the size of the sigma hole, and therefore the strength of the halogen bonding interaction, grew as larger halogens were used for X. This is shown in Figure 2.

For the complexes where halogen bonding seemed possible based on the interaction angles, analysis of the X-Y separation gave more insight into the actual existence of a halogen bond. This analysis was done in the same way as Tawfik and Donald<sup>11</sup>, by comparing the sum of the van der Waals (vdW) radii for  $\text{X}=\text{Cl}$  ( $1.81 \text{ \AA}$ ),

Br (1.95 Å), I (2.15 Å), C(1.85 Å), N (1.54 Å), O (1.40 Å), S (1.85 Å), and Se (2.00 Å). In general, this analysis found optimized distances were shorter than those of the vdW radii, validating the presence of halogen bonding or some other stabilizing interaction between the molecules. Exceptions to this are discussed individually in later sections.

**Table 2:** Computed MH<sub>3</sub>X-Y Bond Angles (Degrees) (M=C, Si, Ge, Sn, Pb; X= F, Cl, Br, I) for the Optimized Halogen Bonding Interactions: *Optimized bond angles between the Lewis acid and Lewis base were measured in degrees. The atoms used to measure the angle were the center atom on the Lewis acid (M), the halogen attached the Lewis acid (X), and the atom on the Lewis base containing the lone electron pair (Y). A hyphen (-) indicates complexes omitted from this study.*

	CH <sub>3</sub> F	CH <sub>3</sub> Cl	CH <sub>3</sub> Br	CH <sub>3</sub> I	SiH <sub>3</sub> I	GeH <sub>3</sub> I	SnH <sub>3</sub> I	PbH <sub>3</sub> I
H <sub>2</sub> O	92.9	67.5	70.4	173.4	169.8	167.8	157.9	152.5
H <sub>2</sub> S	97.5	77.2	74.2	173.6	149.5	149.7	67.4	66.2
H <sub>2</sub> Se	97.2	78.1	74.8	74.8	69.4	69.3	166.5	70.4
THF	-	171.8	172.1	174.5	171.5	172.1	171.4	170.9
furan	73.3	168.4	169.6	-	170.8	171.1	169.6	168.6
CH <sub>3</sub> OCH <sub>3</sub>	75.3	170.5	171.6	174.6	171.9	172.4	171.4	170.9
pyridine	68.4	169.0	171.1	178.8	172.5	173.0	48.4	172.2
F-py	87.0	-	100.4	-	97.4	-	-	-
NH <sub>3</sub>	87.8	158.9	167.7	180.0	180.0	180.0	180.0	180.0
N(CH <sub>3</sub> ) <sub>3</sub>	73.2	171.5	180.0	180.0	180.0	180.0	179.9	180.0
NF <sub>3</sub>	92.9	159.7	165.5	-	166.4	180.0	164.4	162.5
NCl <sub>3</sub>	83.0	170.5	180.0	180.0	180.0	180.0	180.0	179.9
NBr <sub>3</sub>	116.3	172.1	180.0	180.0	180.0	180.0	180.0	180.0

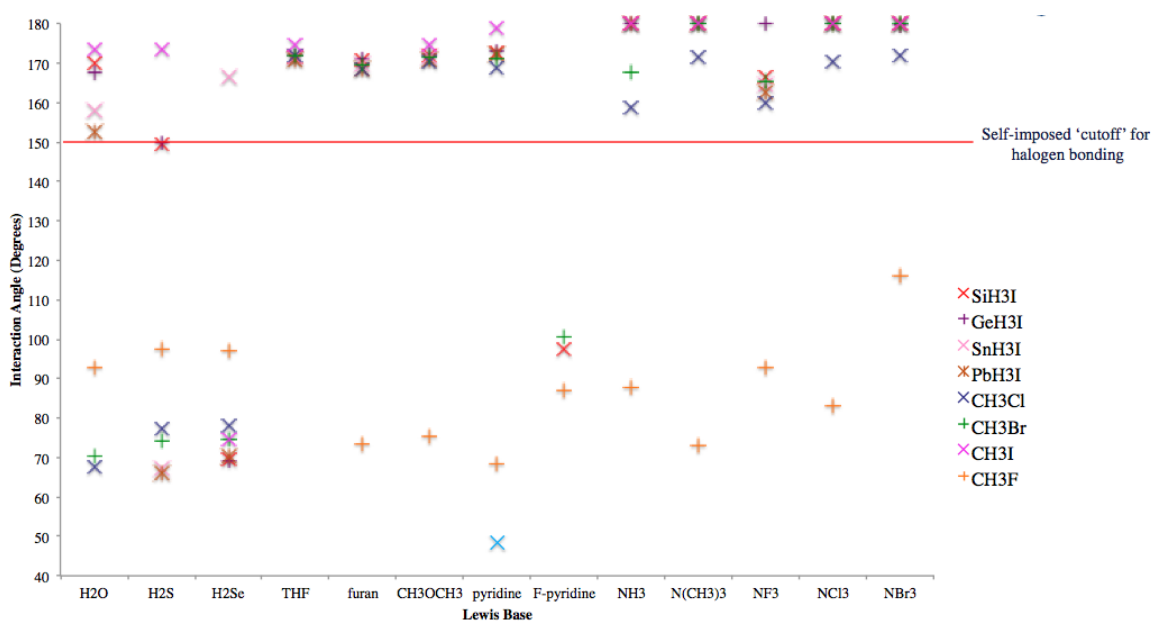


**Figure 3:** Interaction Angles (Degrees) vs. Lewis Base: *This shows the same data visually that was given in Table 2. The red line refers to 150° interaction angles, which was the self-imposed cut off for considering if the complexes formed halogen bonds.*

It should also be noted that not all the molecules tested had successfully optimized by the time of this report. These molecules had their data removed from all the geometric analysis tables. They are still briefly discussed in a later section (Section 3.3).

**Table 3:** Computed R-X---Y Bond Distances for the Optimized Halogen Bonding Interactions Considered in This Work: Bond distances for complexes were listed in angstroms. Complexes that were determined not to exhibit halogen bonding behavior based on their bond angles were left out since this work was focused on halogen bonding and not other forms of interactions. A hyphen (-) indicates molecules with bond angles less than 150° that were omitted. A hyphen (-) indicates complexes omitted from this study.

	CH <sub>3</sub> F	CH <sub>3</sub> Cl	CH <sub>3</sub> Br	CH <sub>3</sub> I	SiH <sub>3</sub> I	GeH <sub>3</sub> I	SnH <sub>3</sub> I	PbH <sub>3</sub> I
H <sub>2</sub> O	-	-	-	3.195	3.399	3.407	3.532	3.598
H <sub>2</sub> S	-	-	-	3.707	3.839	3.818	-	-
H <sub>2</sub> Se	-	-	-	-	-	-	4.015	-
THF	-	3.102	3.012	3.011	3.185	3.169	3.214	3.214
furan	-	3.182	3.122	-	3.307	3.293	3.341	3.355
CH <sub>3</sub> OCH <sub>3</sub>	-	3.100	3.013	3.035	3.207	3.188	3.232	3.229
pyridine	-	3.184	3.058	3.010	3.234	3.202	-	3.217
F-py	-	-	-	-	-	-	-	-
NH <sub>3</sub>	-	3.286	3.177	3.127	3.354	3.320	3.364	3.336
N(CH <sub>3</sub> ) <sub>3</sub>	-	3.083	2.901	2.909	3.120	3.079	3.108	3.058
NF <sub>3</sub>	-	3.299	3.315	-	3.580	3.020	3.598	3.604
NCl <sub>3</sub>	-	3.098	3.028	3.028	3.238	3.213	3.237	3.221
NBr <sub>3</sub>	-	2.998	2.932	3.001	3.127	3.101	3.117	3.093

Stability of the complexes was measured quantitatively with interaction energies. As was done by Tawfik and Donald<sup>11</sup>, zero-point energies were determined at a MP2(Full) level of theory using Gaussian 09. After the initial calculations, counterpoise corrections were applied, again at a MP2(Full) level of theory. These energies can be found in Table 4. Generally, the interactions were found to be stable, but there were exceptions that are discussed individually in later sections.

**3.2 Analysis of Possible Halogen Bonding.** Although the presence of a halogen bond cannot be determined simply by looking at bond angles and interaction distances, broad generalizations can be done, as was done in this work,

to eliminate some of the 144 complexes and say that they definitely do not have a halogen bond. Thus, individual assessments were required to confirm whether or not halogen bonding was occurring in those complexes who formed interactions above the self imposed cut off of 150°. These analyses focused on whether or not a stable interaction formed between the two molecules in the complexes and whether or not the Lewis base interacted directly with the sigma hole at the optimized geometry.

**Table 4:** Zero-Point Energy Adjusted Interaction Energies: *Zero-point energy adjusted interaction energies for all complexes were given in kcal/mol. All energies were calculated at an MP2(full) level of theory and underwent counterpoise corrections.*

	CH <sub>3</sub> F	CH <sub>3</sub> Cl	CH <sub>3</sub> Br	CH <sub>3</sub> I	SiH <sub>3</sub> I	GeH <sub>3</sub> I	SnH <sub>3</sub> I	PbH <sub>3</sub> I
H <sub>2</sub> O	-1.18	-1.53	-1.25	-0.38	0.03	0.10	0.13	-0.10
H <sub>2</sub> S	-0.71	-1.06	-1.03	-0.77	-0.41	-0.42	-1.15	-1.58
H <sub>2</sub> Se	-0.41	-0.77	-0.81	-0.80	-0.68	-0.89	-0.53	-1.38
THF	-	-0.96	-1.48	-2.63	-2.02	-2.00	-1.85	-1.81
Furan	-1.20	-0.54	-0.79	-	-1.06	-1.05	-0.99	-0.97
CH <sub>3</sub> OCH <sub>3</sub>	-1.19	-0.52	-1.01	-2.00	-1.44	-1.40	-1.24	-1.18
Pyridine-(H)	-1.75	-0.42	-1.22	-2.85	-1.91	-1.87	-	-1.52
Pyridine-(F)	-2.15	-	-5.52	-	-2.31	-	-	-
NH <sub>3</sub>	-1.00	0.10	-0.14	-1.52	-0.88	-0.79	-0.54	-0.39
N(CH <sub>3</sub> ) <sub>3</sub>	-1.66	-0.79	-1.87	-3.87	-2.49	-2.52	-4.48	-2.24
NF <sub>3</sub>	-0.04	-0.17	-0.17	-	-0.19	-0.20	-0.21	-0.24
NCl <sub>3</sub>	-0.42	-0.61	-1.06	-1.75	-1.46	-1.46	-1.40	-1.39
NBr <sub>3</sub>	0.09	-0.84	-1.40	-2.31	-1.94	-1.97	-1.89	-1.94

**3.2.1. CH<sub>3</sub>F.** As shown in Table 2 and Figure 3, it was clear that no halogen bonds formed with CH<sub>3</sub>F acting as the Lewis acid, but this was not surprising. Without the presence of electron withdrawing groups on CH<sub>3</sub>F and the high electronegativity of the F atom, no sigma hole developed, as indicated in Figure 2a by the lack of a positive area on the F atom. Without the hole, halogen bonding is extremely weak or non-existent and instead the complexes tended to form those like the ones in Figure 4. Complexes of this form were not halogen bonding, since

there was no sigma hole to interact directly with the Lewis base. In most cases with  $\text{CH}_3\text{F}$ , the Lewis base was interacting with a H atom in  $\text{CH}_3\text{F}$  (Figure 4a).

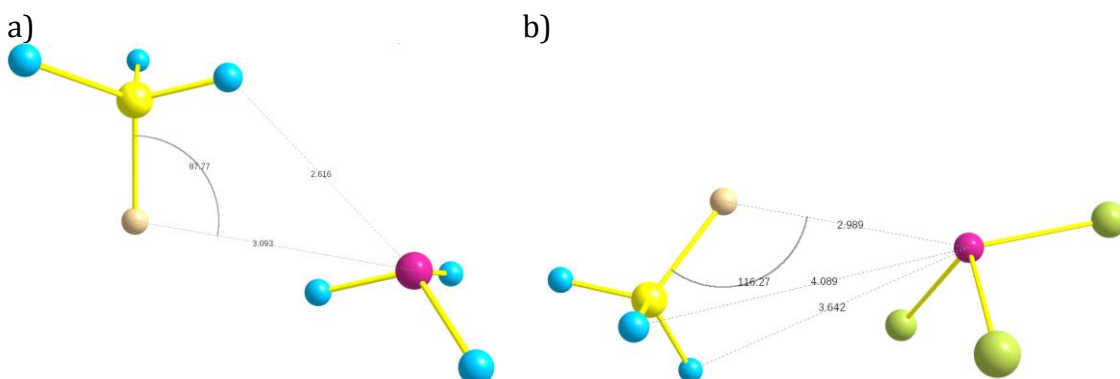


**Figure 4:** Geometric Analysis of  $\text{CH}_3\text{F}-\text{NH}_3$  and  $\text{CH}_3\text{F}-\text{NBr}_3$ : (a) The optimized geometry of  $\text{CH}_3\text{F}-\text{NH}_3$ . With the nonlinear bond angle between  $\text{H}_3\text{CF}---\text{NH}_3$ , this complex was not exhibited halogen bonding behavior. The smaller distance (given in Å) between the N atom and one of the H atoms in  $\text{CH}_3\text{F}$  suggests it was instead interacting with the positive dipole of the H atom. (b) This shows the optimized geometry of  $\text{CH}_3\text{F}-\text{NBr}_3$ . Although not linear, some interaction does appear to be occurring between the halogen and the Lewis base. These were generated and labeled in ChemCraft software.

The one exception was  $\text{CH}_3\text{F}-\text{NBr}_3$ , which did optimize to the largest bond angle ( $116.266^\circ$ ) shown in Figure 4b. Though it not have the  $180^\circ$  of a typical halogen bond, there did appear to be some interaction between the halogen on  $\text{CH}_3\text{F}$  and the lone pair on  $\text{NH}_3$ . This case differed from  $\text{CH}_3\text{F}-\text{NH}_3$  because the halogen and the N atom had a smaller interaction distance than the halogen did with any of the Br atoms. However the large angle prevented the N atom from interacting with the sigma hole, if there even was one, so it was unlikely this was a halogen bond. An electrostatic surface potential for the complex, shown in Figure 5a, revealed that the negative potential on the N atom was interacting with the positive potential on a H atom.

This was different than with  $\text{NBr}_3$ , shown in Figure 5b, where there was still negative potential on the N atom, but the higher electronegativity of the Br atoms

caused a less negative potential to develop on the N atom. Additionally, areas of relative positive potential developed in the cavities between the Br atoms on  $\text{NBr}_3$ . These could have stabilized the negative potential of F in the configuration that the complex optimized to, as the geometry appeared to place the F atom in one of those cavities, which were not present with  $\text{NH}_3$ .

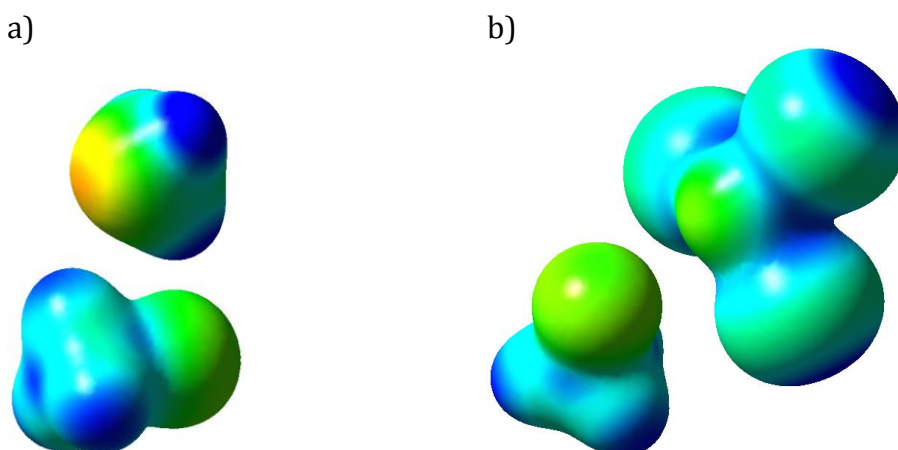


**Figure 5:** Electrostatic Potentials (ESPs) for  $\text{CH}_3\text{F-NH}_3$  and  $\text{CH}_3\text{F-NBr}_3$ : Computed ESP map on the 0.02 iso-density surface for  $\text{CH}_3\text{F}$  with a)  $\text{NH}_3$ , b)  $\text{NBr}_3$ . The ESPs on the surface shown were in the range  $\pm 1.50 \times 10^{-1}$  au, where areas of red were the most negative and areas of blue were the most positive.

**3.2.2.  $\text{CH}_3\text{Cl}$ .** While there were no possible halogen bonding instances found with  $\text{CH}_3\text{F}$ ,  $\text{CH}_3\text{Cl}$  did result with some candidates. Many of the Lewis bases formed complexes with angles greater than  $150^\circ$ , but none reached the ideal  $180^\circ$  that was optimal for halogen bonding. The closest to  $180^\circ$  were  $\text{NX}_3$ , where  $\text{X}=\text{Cl}$ ,  $\text{Br}$ ,  $\text{CH}_3$ , and THF and  $\text{CH}_3\text{OCH}_3$ . With those of the form  $\text{NX}_3$ , this was not surprising. As shown in Figure 6, the N atoms were electronegative and could draw the electron density towards itself, which along with its lone electron pair, could interact well with the sigma hole formed on Cl, even if that hole was small as shown in Figure 2b.



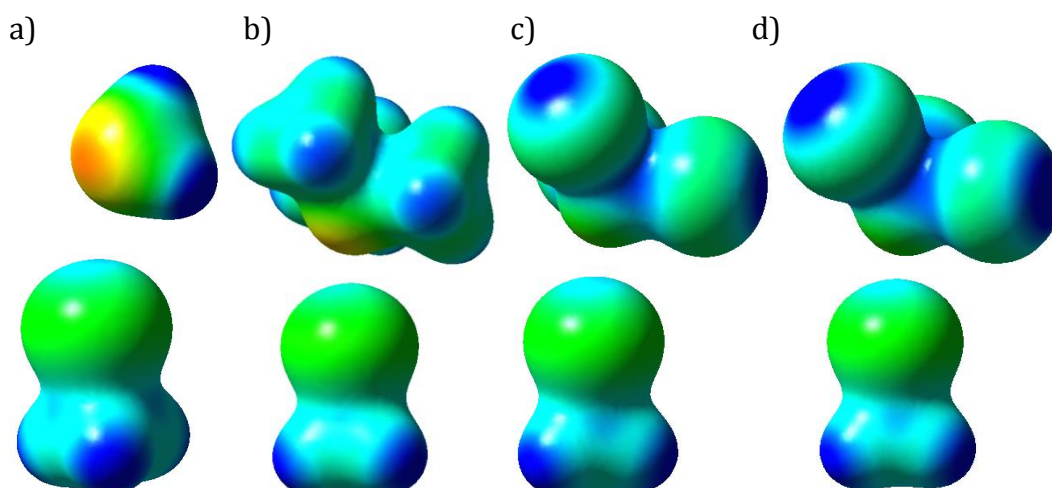


**Figure 6:** ESPs of  $\text{CH}_3\text{Cl-NR}'_3$  ( $\text{R}' = \text{H, Cl, Br, and CH}_3$ ): Computed ESP map on the 0.02 iso-density surface for  $\text{CH}_3\text{Cl}$  with a)  $\text{NH}_3$ , b)  $\text{N}(\text{CH}_3)_3$ , c)  $\text{NCl}_3$ , and d)  $\text{NBr}_3$ . The ESPs on the surface shown were in the range  $\pm 1.50 \times 10^{-1}$  au, where areas of red were the most negative and areas of blue were the most positive.

The Lewis bases, especially  $\text{NH}_3$ , seemed to be tilt away from the sigma hole, which indicated that some other interaction is present. Looking at their geometries (Figure 7), it was apparent that the halogen bonding increased as X went from H to Br, which was an expected trend noticed previously by Tawfik and Donald.<sup>11</sup> With  $\text{NH}_3$ , the Lewis base was positioned so that its H atoms, not the N atom, were closer to the Cl atom on  $\text{CH}_3\text{Cl}$ . Thus, the positive hydrogen, shown in Figures 6a and 7a, were interacting with the area of negative potential of the Cl atom, rather than with the sigma hole. With the lack of an interaction between the sigma hole and the Lewis base, it was determined to not be a halogen bond. Additionally, the zero-point energy (ZPE) adjusted interaction energy of this complex, shown in Table 4, revealed that this interaction was unstable. An interaction with  $\text{NF}_3$  (Not shown), although found to be stable, showed similarities to that of  $\text{CH}_3\text{Cl-NH}_3$  and was also determined to not be a halogen bond.

With  $\text{N}(\text{CH}_3)_3$ , the angle was much larger and the tilt allowed for the hydrogen atoms on two of the methyl groups to move close to the Cl atom. However, the N atom remained the closest to the Cl atom and the orientation allowed for a direct interaction with the sigma hole. Therefore, this was determined to be a halogen bond, but the nonlinear angle suggested that other interactions, possibly with the H atoms on the methyl groups, were stabilizing the complex as well.

With  $\text{NCl}_3$  and  $\text{NBr}_3$ , shown in Figures 6c, 7c, and 6d, 7d, respectively, there were no H atoms that could be stabilized by the electron rich halogen. Rather it appeared as though the sigma hole was the location of the primary interaction. They were still tilted however, which could be due to the areas of positive potential on the Cl and Br atoms, brought on by the electron withdrawing effects of the N atom.

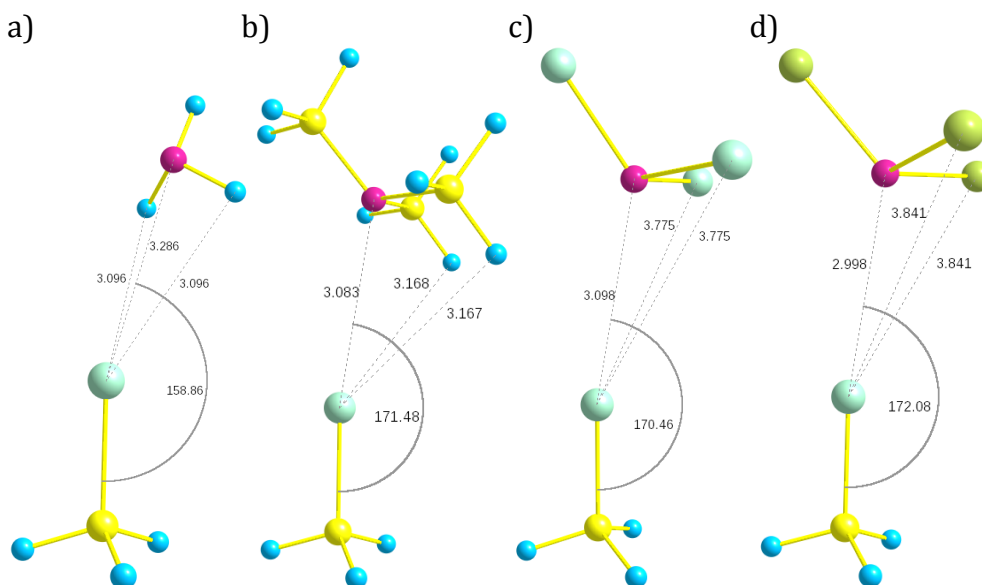


**Figure 7:** Geometric Analysis of  $\text{CH}_3\text{Cl}-\text{NR}'_3$  ( $\text{R}'=\text{H}, \text{Cl}, \text{Br},$  and  $\text{CH}_3$ ): Geometric visualization of  $\text{CH}_3\text{Cl}$  with a)  $\text{NH}_3$ , b)  $\text{N}(\text{CH}_3)_3$ , c)  $\text{NCl}_3$ , and d)  $\text{NBr}_3$ . These were generated and labeled in ChemCraft software.

The positive areas between the N atom and the Br atoms could also have been stabilized by the negative area of the Cl atom, which could only have been contacted with each other via the tilt. The titling of the Lewis base seemed to be an indication of how weak the halogen bonding was with CH<sub>3</sub>Cl, as other interactions must have also been present to stabilize the complexes.

With THF and CH<sub>3</sub>OCH<sub>3</sub>, shown in Figures 8a, 9a and 8b, 9b, respectively, a similar interaction was observed. The molecules tilted in order for one of the lone pairs on the O atom to interact with the sigma hole on the Cl atom. Additionally, this arrangement allowed for the positive H atoms on THF to interact with the negative area on the Cl atom, providing further stabilization. This was indicated by the small distance between the Cl and the H atoms, which was comparable to the distance between the Cl atom and the O atom. Interactions of H atoms with the Cl atom were not seen with CH<sub>3</sub>OCH<sub>3</sub>, and could be the reason that CH<sub>3</sub>OCH<sub>3</sub> formed a less stable complex with an interaction energy of -0.52 kcal/mol, while THF had a ZPE adjusted interaction energy of -0.96 kcal/mol.

Furan and pyridine, shown in Figures 8c, 9c, and 8d, 9d, also showed interaction with the sigma hole. With these molecules, a different geometric preference was favored than with the molecules previously mentioned. Although furan and pyridine tilted from their straight on initial geometry, they only tilted to the side, rather than to the side and back like THF and MeOMe did. This geometry allowed for one of the hydrogen atoms to interact with the negative area of the Cl atom. In fact, the hydrogen atom interacting with the negative area of the Cl atom

was closer to the Cl atom than the N atom interacting with the sigma hole. Again, these showed evidence of how weak the sigma holes on  $\text{CH}_3\text{Cl}$  were.

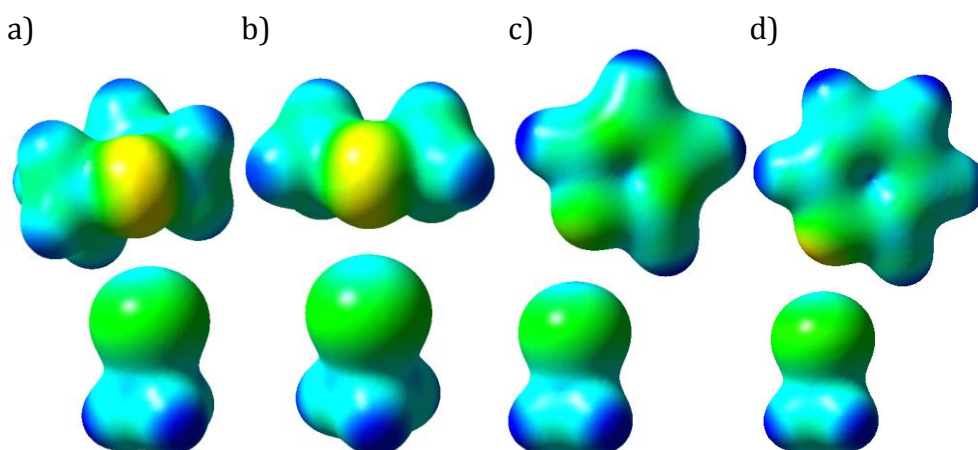


**Figure 8:** ESPs of  $\text{CH}_3\text{Cl}-\text{Y}$  ( $\text{Y}=\text{THF}$ ,  $\text{CH}_3\text{OCH}_3$ , furan, pyridine): Computed ESP map on the 0.02 iso-density surface for  $\text{CH}_3\text{Cl}$  with a) THF b)  $\text{CH}_3\text{OCH}_3$ , c) furan, and d) pyridine. The ESPs on the surface shown were in the range  $\pm 1.50 \times 10^{-1}$  au, where areas of red were the most negative and areas of blue were the most positive.

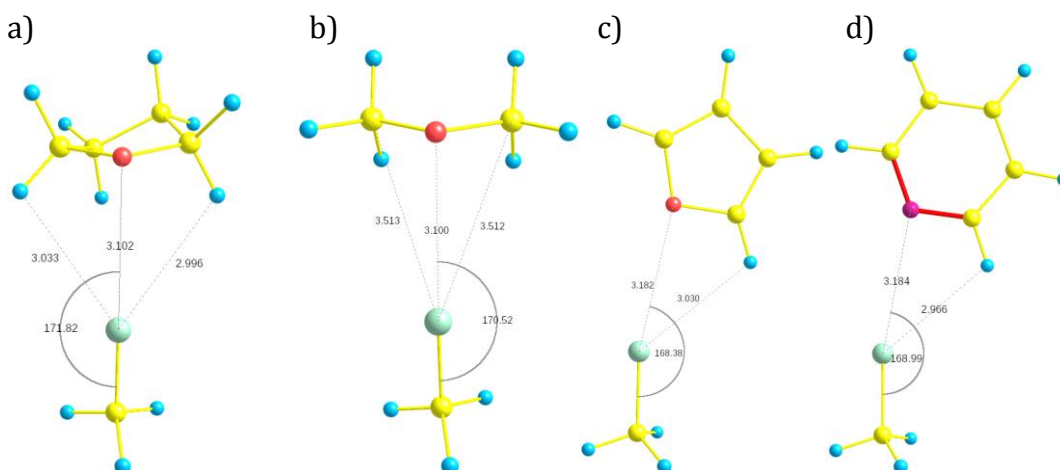


**Figure 9:** Geometric Analysis of  $\text{CH}_3\text{Cl}-\text{Y}$  ( $\text{Y}=\text{THF}$ ,  $\text{CH}_3\text{OCH}_3$ , furan, pyridine): Geometric visualization of  $\text{CH}_3\text{Cl}$  with with a) THF b)  $\text{CH}_3\text{OCH}_3$ , c) furan, and d) pyridine. These were generated and labeled in ChemCraft software.

Overall, it was found that halogen bonding was occurring with 7 Lewis bases:  $\text{N}(\text{CH}_3)_3$ ,  $\text{NCl}_3$ ,  $\text{NBr}_3$ , THF,  $\text{CH}_3\text{OCH}_3$ , furan, and Pyridine-F. This was a trend with all the Lewis acids tested in this work. Additionally, none of the molecules

formed linear conformations with  $\text{CH}_3\text{Cl}$ , a testament to the weak nature of the sigma hole on these Lewis acids.

**3.2.3.  $\text{CH}_3\text{Br}$ .**  $\text{CH}_3\text{Br}$  showed possible halogen bonding with all the same molecules as  $\text{CH}_3\text{Cl}$ . This was not be a surprise because Br provided a better sigma hole to halogen bond with, as was shown in Figure 2c. This sigma hole allowed stronger halogen bonds than those seen with  $\text{CH}_3\text{Cl}$ , shown by larger angles of interaction and more negative interaction energies, with  $\text{CH}_3\text{F}$  being an exception.  $\text{CH}_3\text{Br}$  successfully produced three ideal examples of halogen bonding by forming complexes with bond angles of  $180^\circ$  with  $\text{N}(\text{CH}_3)_3$ ,  $\text{NCl}_3$ , and  $\text{NBr}_3$ , shown below in Figures (10,11a), (10,11)b, and (10,11)d, respectively.

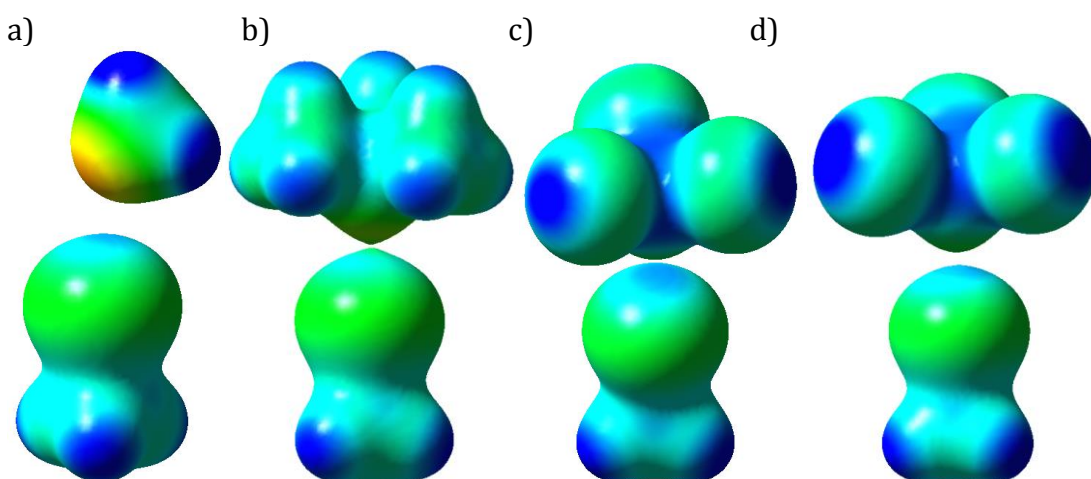


**Figure Number 10:** ESPs for  $\text{CH}_3\text{Br-NR}'_3$  ( $\text{R}'=\text{H, CH}_3, \text{Cl, Br}$ ): Computed ESP map on the 0.02 isodensity surface for  $\text{CH}_3\text{Br}$  with a)  $\text{NH}_3$ , b)  $\text{N}(\text{CH}_3)_3$ ,  $\text{NCl}_3$ , and d)  $\text{NBr}_3$ . The ESPs on the surface shown were in the range  $\pm 1.50 \times 10^{-1}$  au, where areas of red were the most negative and areas of blue were the most positive.

The  $180^\circ$  angles and short bond distances showed the difference halogen bonding makes. These distances were shorter than their van der Waals equivalents, and the interaction allowed two atoms, generally thought of as both negatively charged, to directly face towards each other. Even with larger atoms, the two molecules

approached each other closer than they did when a Cl atom was on the Lewis acid. Thus, the larger sigma hole produced by the Br atom produced quite a difference when compared to the interactions caused by the Cl atom's sigma hole.

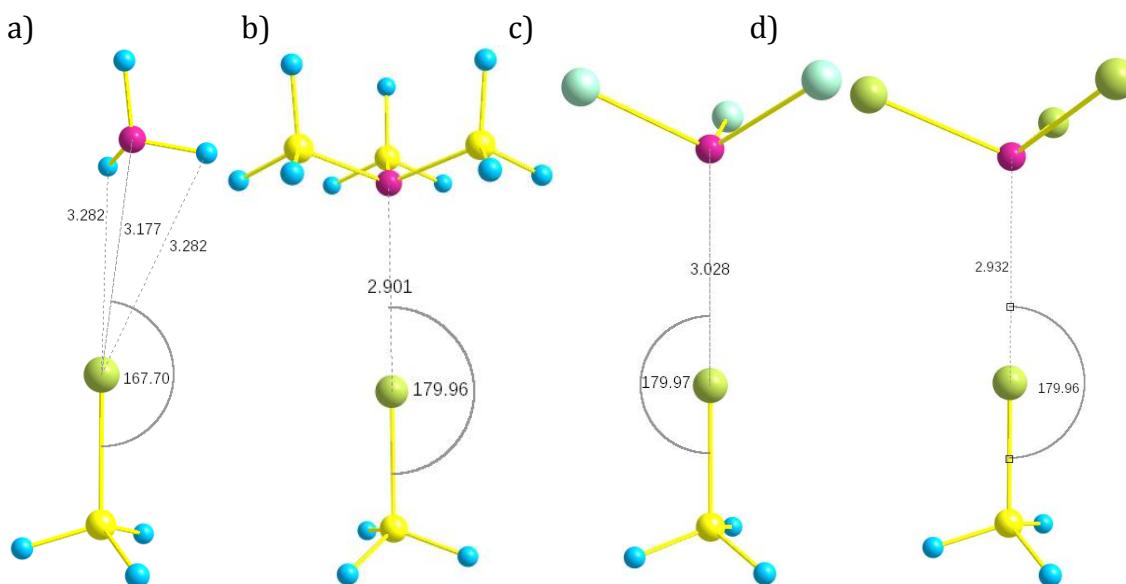


**Figure Number 11:** Geometric Analysis of  $\text{CH}_3\text{Br}-\text{NR}'_3$  ( $\text{R}'=\text{H}, \text{CH}_3, \text{Cl}, \text{Br}$ ): Geometric visualization of  $\text{CH}_3\text{Br}$  with a)  $\text{NH}_3$ , b)  $\text{N}(\text{CH}_3)_3$ ,  $\text{NCl}_3$ , and d)  $\text{NBr}_3$ . These were generated and labeled in ChemCraft software.

These differences were not limited to just the linear halogen bonds detailed above. Also included in Figures 10a and 11a was the interaction with  $\text{NH}_3$ . With  $\text{CH}_3\text{Cl}$ , it was observed that the  $\text{NH}_3$  did not halogen bond with the Lewis acid. With Br's sigma hole, a different interaction was observed. The  $\text{NH}_3$  remained tilted, but the N atom approached the Br atom closer than the H atoms. This was also accompanied with an increase in interaction angle by  $10^\circ$ . This larger angle allowed for the N atom to interact with the sigma hole and produce a halogen bond. This interaction produced a distance smaller than the sum of van der Waals radii and a distance smaller than was observed between  $\text{NH}_3$  and  $\text{CH}_3\text{Cl}$ . Additionally, the

interaction was stable, as shown by the ZPE adjusted interaction energy in Table 4. As with  $\text{CH}_3\text{Cl}$ , an interaction similar to  $\text{CH}_3\text{Br-NH}_3$  was seen with  $\text{CH}_3\text{Br-NF}_3$ .

The increased halogen bonding character was also reflected with the other Lewis bases. THF,  $\text{CH}_3\text{OCH}_3$ , furan, and pyridine, shown in Figures 12 and 13, once again showed the possibility for halogen bonding with their larger bond angles. With a quick glance these complexes looked identical to those formed with  $\text{CH}_3\text{Cl}$ , and that was because they were. THF,  $\text{CH}_3\text{OCH}_3$ , furan, and pyridine interacted exactly the same way as they did with the previous Lewis acid. The angles of interaction increased slightly due to the larger sigma hole, but generally they formed almost identical geometric preferences. While similar, the zero point interaction energies, shown in Table 4, indicated that overall, the interactions were more stable than those with  $\text{CH}_3\text{Cl}$ , brought on by stronger attraction with the larger sigma hole.

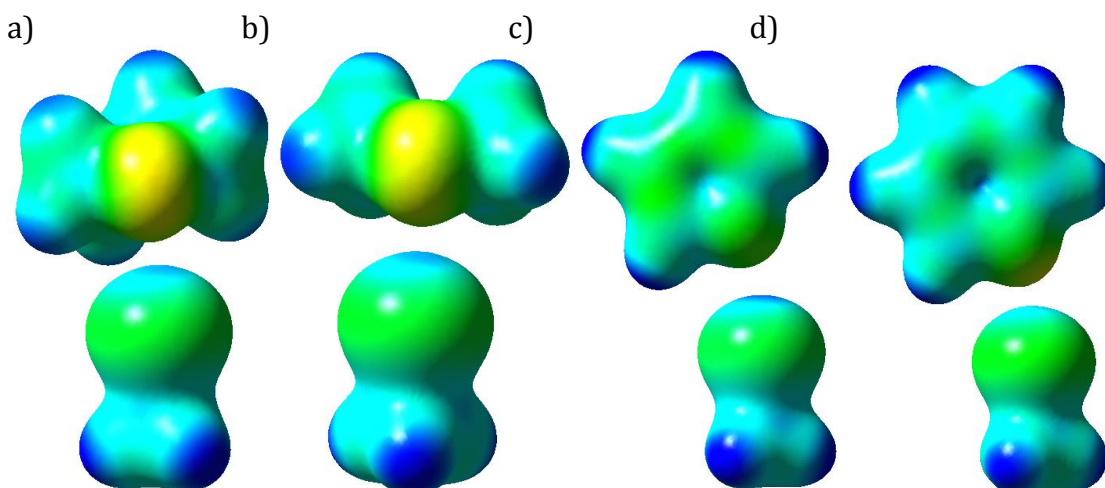


**Figure 12:** ESPs for  $\text{CH}_3\text{Br-Y}$  ( $\text{Y}=\text{THF}$ ,  $\text{CH}_3\text{OCH}_3$ , furan, and pyridine): *Computed ESP map on the 0.02 iso-density surface for  $\text{CH}_3\text{Br}$  with a) THF b)  $\text{CH}_3\text{OCH}_3$ , c) furan, and d) pyridine. The ESPs on the surface shown were in the range  $\pm 1.50 \times 10^{-1}$  au, where areas of red were the most negative and areas of blue were the most positive.*

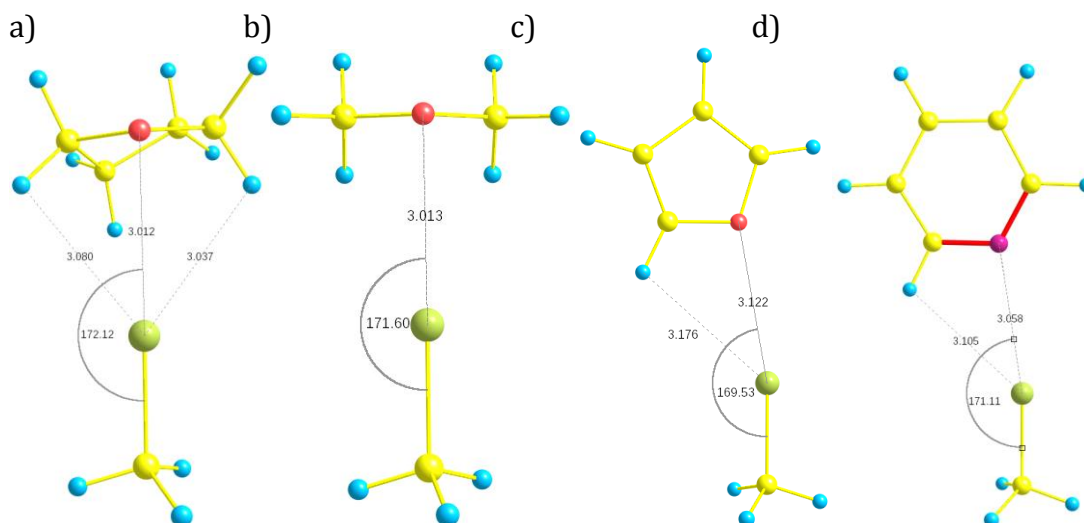


**Figure 13:** Geometric Analysis of  $\text{CH}_3\text{Br}-\text{Y}$  ( $\text{Y}=\text{THF}$ ,  $\text{CH}_3\text{OCH}_3$ , furan, and pyridine): Geometric visualization of  $\text{CH}_3\text{Br}$  with with a) *THF* b) *CH<sub>3</sub>OCH<sub>3</sub>*, c) *furan*, and d) *pyridine*. These were generated and labeled in ChemCraft software.

Overall,  $\text{CH}_3\text{Br}$  produced stronger, more linear halogen bonding with the same molecules that were looked at with  $\text{CH}_3\text{Cl}$ . Their general geometric arrangements also maintained the same form for the most part. Thus, the larger sigma hole on Br was able to produce stronger halogen bonding, which allowed it to form halogen bond interactions with  $\text{NH}_3$  and  $\text{NF}_3$ .

**3.2.4.  $\text{CH}_3\text{I}$ .** It had previously been established that  $\text{CH}_3\text{I}$  produces the largest sigma hole<sup>10</sup> so it comes as no surprise that the interactions with the sigma hole on  $\text{CH}_3\text{I}$  produced the most stable interactions, evident by comparing the zero-point interaction energies in Table 4. Because of this, any of the Lewis bases that previously showed affinity for halogen bonding interacted with  $\text{CH}_3\text{I}$  in the same way they did with the other Lewis acids studied thus far, but with shorter distances and angles closer to  $180^\circ$ .  $\text{N}(\text{CH}_3)_3$ ,  $\text{NCl}_3$ , and  $\text{NBr}_3$  once again produced  $180^\circ$  bond angles, as was seen with  $\text{CH}_3\text{Br}$ . Additionally,  $\text{NH}_3$ , shown below in Figure 14, also formed a complex with a bond angle of  $180^\circ$ . This linear interaction was brought on



by the larger sigma hole. When the sigma hole was smaller, the interaction was not as strong so an interaction between H atoms on  $\text{NH}_3$  and the halogen was necessary to stabilize the complex. With  $\text{CH}_3\text{I}$ , the sigma hole was large enough to stabilize the complex entirely by itself.

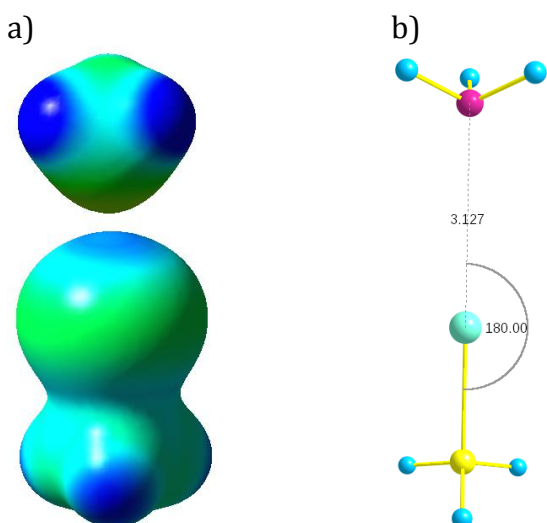


**Figure Number 14:** ESP and Geometric Analysis of  $\text{CH}_3\text{I}-\text{NH}_3$ : a) Computed ESP map on the 0.02 iso-density surface for  $\text{CH}_3\text{I}$  with  $\text{NH}_3$ . The ESP on the surface shown were in the range  $\pm 1.50 \times 10^{-1}$  au, where areas of red were the most negative and areas of blue were the most positive. b) Geometric visualization of  $\text{CH}_3\text{I}$  with  $\text{NH}_3$ . This was generated and labeled in ChemCraft software.

Another change from what was seen with other Lewis acids was the interaction with pyridine, shown below in Figure 15. Whereas with the previously analyzed Lewis bases, the pyridine interacted sideways with the sigma hole. With  $\text{CH}_3\text{I}$ , the entire interaction was between the halogen and the N atom. This nearly linear interaction showed a halogen bond stabilizing the complex in a way not seen with  $\text{CH}_3\text{F}$ ,  $\text{CH}_3\text{Cl}$ , or  $\text{CH}_3\text{Br}$ .

In addition to Lewis bases that previously halogen bonded with the Lewis acids studied so far,  $\text{CH}_3\text{I}$  showed halogen bonding character with  $\text{H}_2\text{O}$  and  $\text{H}_2\text{S}$ , shown below in Figure 16. Because of requiring O or S to interact with the sigma

hole, these molecules tilted themselves similar to the ways in which THF and  $\text{CH}_3\text{OCH}_3$  tilted.

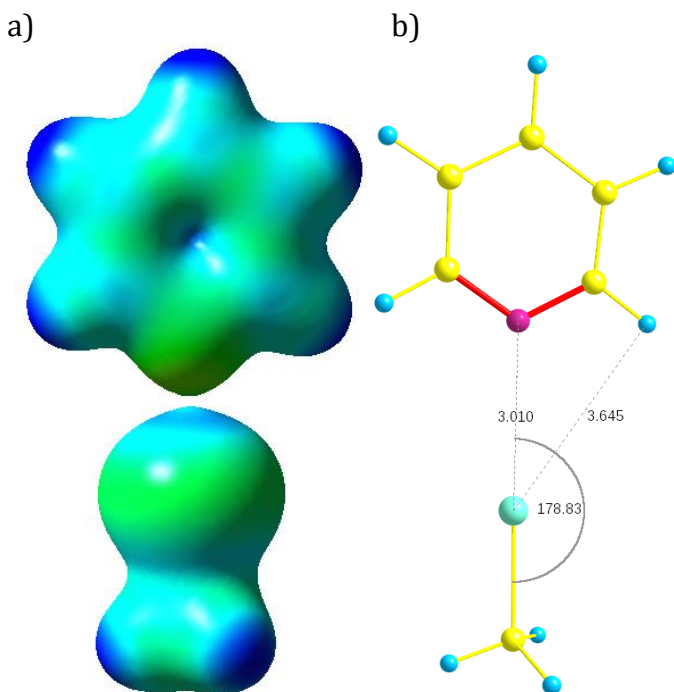


**Figure Number 15:** ESP and Geometric Analysis of  $\text{CH}_3\text{I}$ -pyridine: a) Computed electrostatic potential (ESP) map on the 0.02 iso-density surface for  $\text{CH}_3\text{I}$  with pyridine. The ESP on the surface shown were in the range  $\pm 1.50 \times 10^{-1}$  au, where areas of red were the most negative and areas of blue were the most positive. b) Geometric visualization of  $\text{CH}_3\text{I}$  with with pyridine. This was generated and labeled in ChemCraft software.

Previously, the reason that  $\text{H}_2\text{O}$  and  $\text{H}_2\text{S}$  had not formed linear bonds to be considered for halogen bonding was due to the fact the smaller sigma holes allowed for hydrogen bonding to dominate the interaction between the two molecules. With the stronger sigma hole on  $\text{CH}_3\text{I}$ , halogen bonding was capable of stabilizing the molecule instead, but there appeared to still be some hydrogen bonding at work. With  $\text{H}_2\text{O}$ , the hydrogen atoms were significantly farther away than the O atom to the sigma hole on  $\text{CH}_3\text{I}$ , which supports the idea that halogen bonding was the dominant stabilizing interaction. However with  $\text{H}_2\text{S}$ , the hydrogen atoms were only

slightly farther. This was an indication that as halogen bonding decreased, hydrogen bonding increased to make up for the loss of stabilization. This decrease in halogen bonding capabilities was due to the fact that oxygen was more electronegative than S, which meant it could develop a larger negative potential than S to interact with the sigma hole, as shown in Figure 16a,c. Thus the halogen bond with H<sub>2</sub>O was stronger, and the interaction shows less hydrogen bonding character.

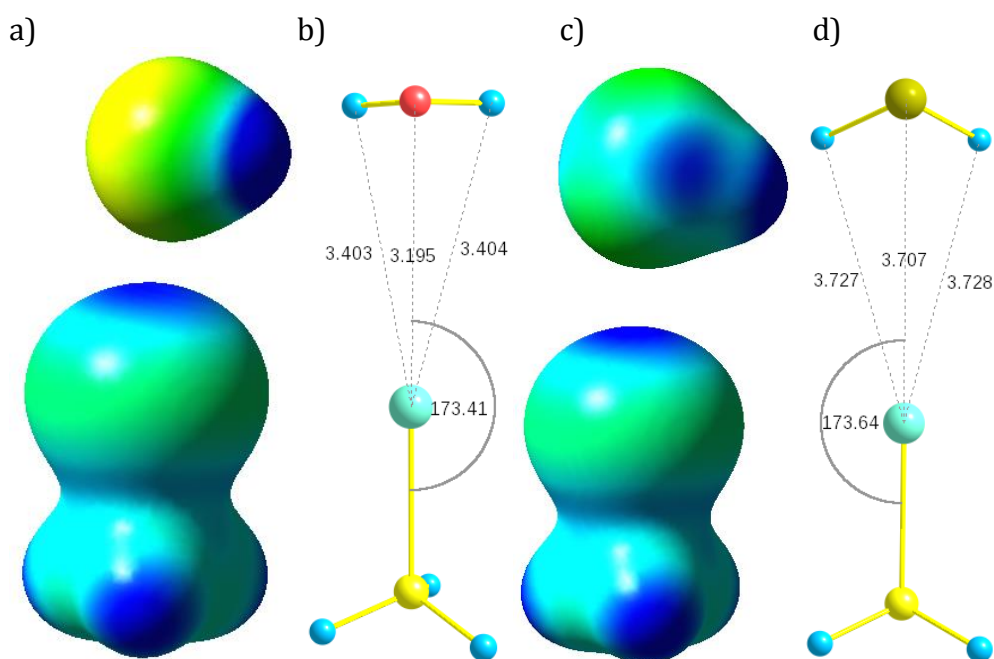


**Figure number 16:** ESPs and Geometric Analysis of CH<sub>3</sub>I-H<sub>2</sub>O and CH<sub>3</sub>I-H<sub>2</sub>S: *a,c*) Computed ESP map on the 0.02 iso-density surface for CH<sub>3</sub>I with *a*) H<sub>2</sub>O and *c*) H<sub>2</sub>S. The ESP on the surface shown were in the range  $\pm 1.50 \times 10^{-1}$  au, where areas of red were the most negative and areas of blue were the most positive. *b,d*) Geometric visualization of CH<sub>3</sub>I with *b*) H<sub>2</sub>O and *e*) H<sub>2</sub>S. These were generated and labeled in ChemCraft software.

With halogen bonding established for CH<sub>3</sub>X, where X=F, Cl, Br, and I, the use of different center atoms on the Lewis acid was examined. Since iodide showed the most affinity for halogen bonding, iodide remained as the halogen involved in the

interaction. Additionally, many of the patterns established already will remain constant with other Lewis acids.

**3.2.5. SiH<sub>3</sub>I.** As expected based on previous research<sup>10,11</sup>, SiH<sub>3</sub>I showed favorability towards forming halogen bonds with various Lewis bases. As was stated earlier, a cutoff of 150° was used to eliminate any complexes that did not form halogen bonds. Of those that met the initial requirement, several of them, shown in Figure 17, reached the ideal 180° needed for a strong halogen bond. The sigma hole on the SiH<sub>3</sub>I was stabilized by the N atom on the Lewis base drawing in the electrons from its substituents and was able to form these geometric preferences.

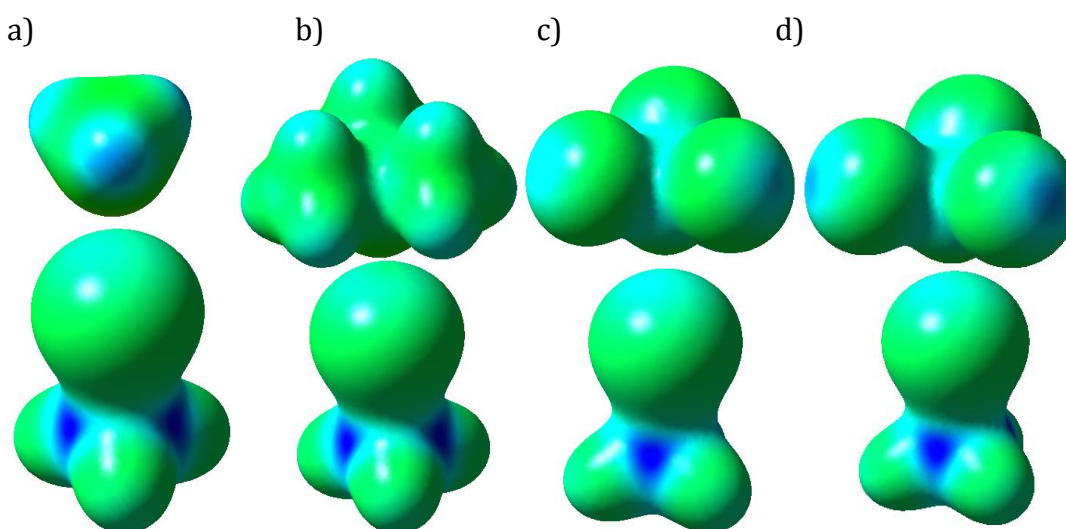


**Figure 17:** ESPs of SiH<sub>3</sub>I-NR'<sub>3</sub> (R'=H, CH<sub>3</sub>, Cl, Br): Computed ESP map on the 0.02 iso-density surface for SiH<sub>3</sub>I with a) NH<sub>3</sub>, b) N(CH<sub>3</sub>)<sub>3</sub>, NCl<sub>3</sub>, and d) NBr<sub>3</sub>. The ESPs on the surface shown were in the range +/- 3.09 x 10<sup>-1</sup> au, where areas of red were the most negative and areas of blue were the most positive.

Forming smaller bond angles, NF<sub>3</sub>, furan, THF, pyridine, and CH<sub>3</sub>OCH<sub>3</sub> still showed halogen bonding like characteristics that were similarly seen with CH<sub>3</sub>I and CH<sub>3</sub>Br (Figures 12,13). In each case, the Lewis base was still interacting directly with the sigma hole, as demonstrated in Figure 18 with furan and CH<sub>3</sub>OCH<sub>3</sub>. This

interaction, similar to the ones shown earlier, produced smaller, nonlinear angles that suggested these halogen bonds were weaker. There were differences between the interaction formed with furan and that with  $\text{CH}_3\text{OCH}_3$ . Figure 19 provides more geometric details and visualizations about these differences. Although their bond angles were similar,  $\text{CH}_3\text{OCH}_3$  and THF interacted more directly with  $\text{SiH}_3\text{I}$  than furan and pyridine.

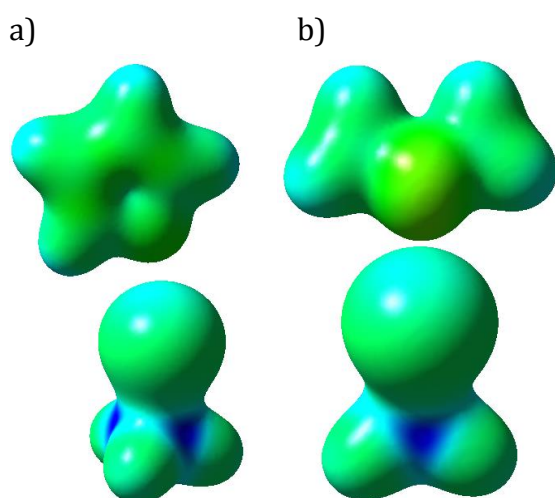


**Figure 18:** ESPs of  $\text{SiH}_3\text{I}$ -furan and  $\text{SiH}_3\text{I}$ - $\text{CH}_3\text{OCH}_3$ : Computed ESP map on the 0.02 iso-density surface for  $\text{SiH}_3\text{I}$  with a) furan and b)  $\text{CH}_3\text{OCH}_3$ . The ESPs on the surface shown were in the range  $\pm 3.09 \times 10^{-1}$  au, where areas of red were the most negative and areas of blue were the most positive.

Furan and pyridine each interacted with the sigma hole with a slight tilt in their orientation rather than straight on, as was seen with  $\text{CH}_3\text{Br}$ . This arrangement allowed for one of their H atoms to get closer to  $\text{SiH}_3\text{I}$ , and particularly, closer to the I atom. As can be seen with furan in Figure 18, the hydrogen atoms had areas of positive electrostatic potential on them.

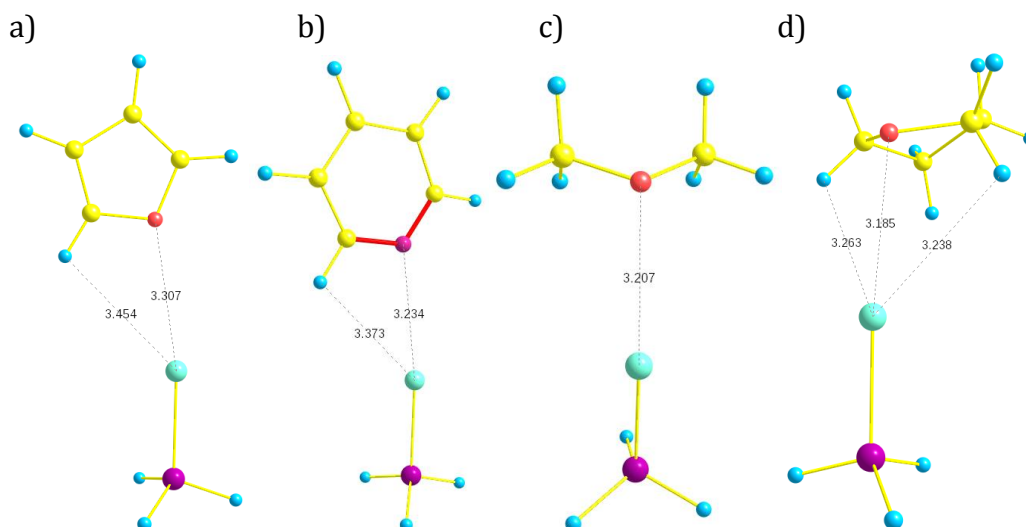


**Figure 19:** Geometric Analysis of  $\text{SiH}_3\text{I}-\text{Y}$  ( $\text{Y}=\text{furan}$ ,  $\text{pyridine}$ ,  $\text{CH}_3\text{OCH}_3$ ,  $\text{THF}$ ): Geometric visualization of  $\text{SiH}_3\text{I}$  with with a) *furan* b) *pyridine*, c) *CH<sub>3</sub>OCH<sub>3</sub>*, and d) *THF*. These were generated and labeled in ChemCraft software.

In Figure 19, the distances between the hydrogen atoms and the I atom were only slightly longer than that of the N atom. The positive density on the H atom could interact with the negative area on the I atom to stabilize the complex. Regardless, the N atom appeared to be halogen bonding with the I atom and was only further stabilized by the interaction between the H and I atoms.

With  $\text{CH}_3\text{OCH}_3$  and  $\text{THF}$  however, the molecules were tilted backwards from the molecule, rather than favoring one side of their substituents. This was due to the fact that an O atom was interacting with the sigma hole. The tilting allowed for one the lone pairs to interact with the sigma hole. This was similar to what was seen by Tawfik and Donald<sup>11</sup> and was seen with these Lewis bases previously.

Unfortunately the interaction energies, listed in Table 4, provides no evidence that either of these interactions was more stable than the other. They did show that  $\text{THF}$  formed the most stable halogen bond with  $-2.02$  kcal/mol interaction

energy while furan formed the weakest with an interaction energy of -1.06 kcal/mol.

As can be seen in Figure 20, H<sub>2</sub>O interacted with the sigma hole on SiH<sub>3</sub>I in a way similar to CH<sub>3</sub>OCH<sub>3</sub> or THF and in a way that was previously seen with CH<sub>3</sub>I. In fact, the bond angle was similar to CH<sub>3</sub>OCH<sub>3</sub> or THF at 169.8°. Oxygen interacting with the sigma hole could have been the cause for these similarities, since the tilt allowed for one of the lone pairs to interact with the sigma hole. The interaction, however, yielded a positive ZPE adjusted interaction energy of 0.03 kcal/mol. This indicated that the interaction was unstable, which suggested that the sigma hole was not strong enough to form a strong halogen bond.

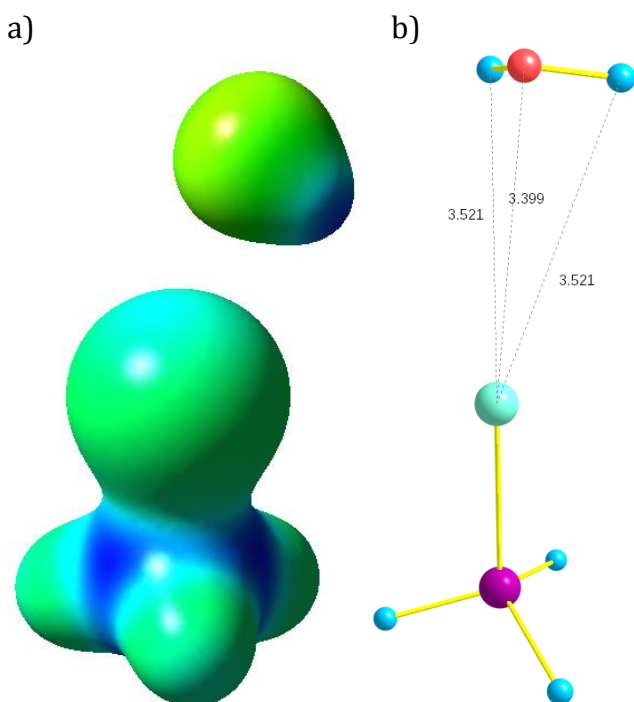


**Figure Number 20:** ESP and Geometric Analysis of SiH<sub>3</sub>I-H<sub>2</sub>O: a) Computed ESP map on the 0.02 iso-density surface for SiH<sub>3</sub>I with H<sub>2</sub>O. The ESPs on the surface shown were in the range  $\pm 3.09 \times 10^{-1}$  au, where areas of red were the most negative and areas of blue were the most positive. b) Geometric visualization of SiH<sub>3</sub>I with H<sub>2</sub>O. This was generated and labeled in ChemCraft software

**3.2.6. GeH<sub>3</sub>I.** GeH<sub>3</sub>I formed interactions similar to those of SiH<sub>3</sub>I with NF<sub>3</sub>, NCl<sub>3</sub>, furan, H<sub>2</sub>O, NBr<sub>3</sub>, N(CH<sub>3</sub>)<sub>3</sub>, CH<sub>3</sub>OCH<sub>3</sub>, pyridine, NH<sub>3</sub>, and THF. Additionally, GeH<sub>3</sub>I formed linear bonds with NF<sub>3</sub>, NH<sub>3</sub>, NCl<sub>3</sub>, NBr<sub>3</sub>, and N(CH<sub>3</sub>)<sub>3</sub>, which are pictured below (excluding NF<sub>3</sub>) in Figure 21.

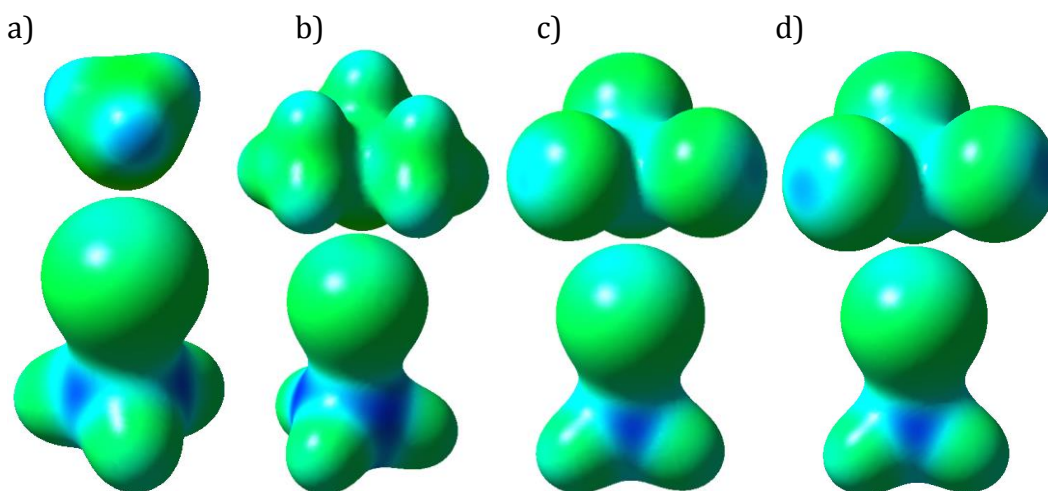


**Figure 21:** ESPs for GeH<sub>3</sub>I-NR'<sub>3</sub> (X=Cl, Br, CH<sub>3</sub>, and H): *Computed ESP map on the 0.02 iso-density surface for GeH<sub>3</sub>I with a)NH<sub>3</sub>, b) N(CH<sub>3</sub>)<sub>3</sub>, NCl<sub>3</sub>, and d) NBr<sub>3</sub>. The ESPs on the surface shown were in the range +/- 3.09 x 10<sup>-1</sup> au, where areas of red were the most negative and areas of blue were the most positive.*

CH<sub>3</sub>OCH<sub>3</sub>, pyridine, furan, and THF, shown in Figure 22, also formed bond angles of around 170° and interacted similarly with GeH<sub>3</sub>I as they did with SiH<sub>3</sub>I. These structures were very similar to those formed with SiH<sub>3</sub>I, shown in Figure 19. As with SiH<sub>3</sub>I, the halogen bonds formed by furan and Pyridine-F relied on interactions with one of the H atoms on the Lewis base, while THF and CH<sub>3</sub>OCH<sub>3</sub> tilted backwards so one of oxygen's lone electron pairs could interact with the sigma hole as well as avoid eclipsing the H atoms on GeH<sub>3</sub>I with its own substituents.



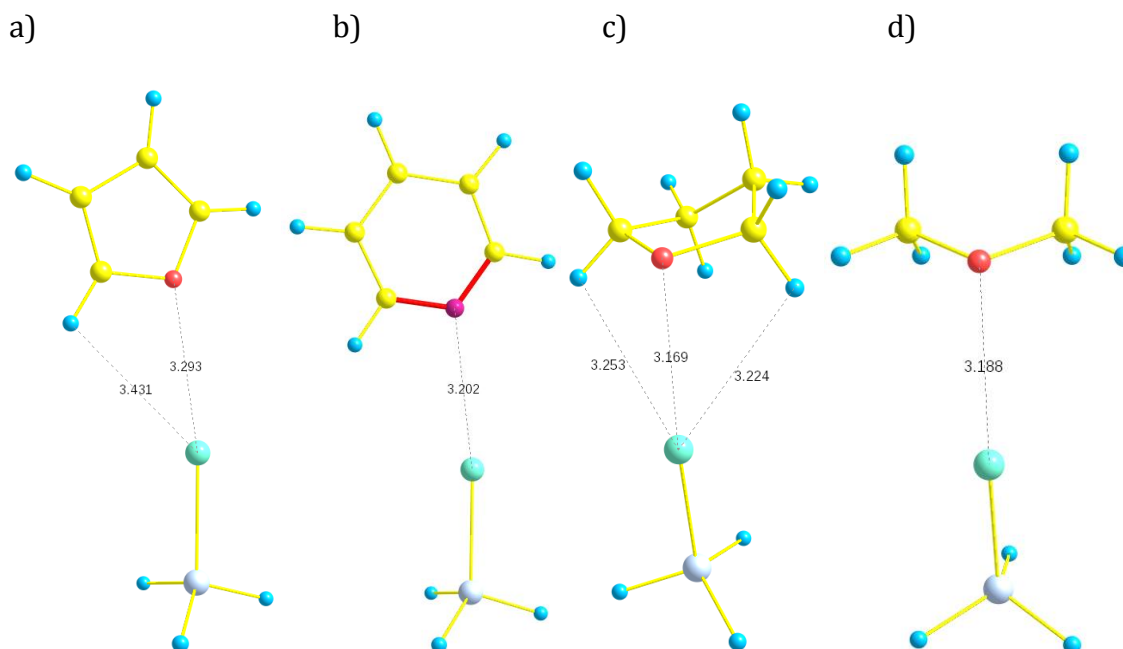


**Figure 22:** Geometric Analysis of  $\text{GeH}_3\text{I}-\text{Y}$  ( $\text{Y}=\text{furan}$ ,  $\text{pyridine}$ ,  $\text{THF}$ , and  $\text{CH}_3\text{OCH}_3$ ): Geometric visualization of  $\text{GeH}_3\text{I}$  with with a)  $\text{furan}$  b)  $\text{pyridine}$ , c)  $\text{H}_3\text{COCH}_3$ , and d)  $\text{THF}$ . These were generated and labeled in ChemCraft software.

In addition to these Lewis bases,  $\text{H}_2\text{O}$ , shown in Figure 23, also formed a complex with  $\text{GeH}_3\text{I}$  in a way similar to how it did with  $\text{SiH}_3\text{I}$ . This geometric configuration, similar to the ones formed by  $\text{THF}$  and  $\text{CH}_3\text{OCH}_3$ , allowed a lone electron pair to interact with the sigma hole. Again, this interaction was energetically unfavorable with a ZPE adjusted interaction energy of  $+0.10$  kcal/mol, suggesting that the sigma hole was not strong enough to make this interaction stable.

**3.2.7.  $\text{SnH}_3\text{I}$ .** Looking at  $\text{SnH}_3\text{I}$  complex bond angles,  $\text{NF}_3$ ,  $\text{NCl}_3$ ,  $\text{furan}$ ,  $\text{SeH}_2$ ,  $\text{H}_2\text{O}$ ,  $\text{NBr}_3$ ,  $\text{N}(\text{CH}_3)_3$ ,  $\text{CH}_3\text{OCH}_3$ ,  $\text{NH}_3$ , and  $\text{THF}$  had possible halogen bonding, as was seen with the previous Lewis acids studied. Again,  $\text{NCl}_3$ ,  $\text{NH}_3$ ,  $\text{NBr}_3$ , and  $\text{N}(\text{CH}_3)_3$  were the Lewis bases that showed the strongest evidence for halogen bonding, based on their  $180^\circ$  bond angles.

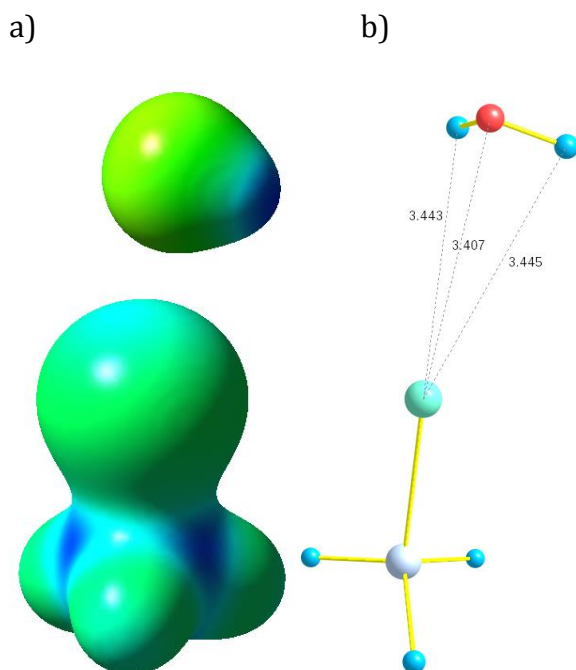


**Figure 23:** ESP and Geometric Analysis of  $\text{GeH}_3\text{I}-\text{H}_2\text{O}$ : a) Computed ESP map on the 0.02 iso-density surface for  $\text{GeH}_3\text{I}$  with  $\text{H}_2\text{O}$ . The ESPs on the surface shown were in the range  $\pm 3.09 \times 10^{-1}$  au, where areas of red were the most negative and areas of blue were the most positive. b) Geometric visualization of  $\text{GeH}_3\text{I}$  with  $\text{H}_2\text{O}$ . This was generated and labeled in ChemCraft software

Looking at their ESPs, Figure 24, it was clear that these interactions were the same as they were with previous Lewis acids. Looking at their interaction energies in Table 4, these were weaker than  $\text{SiH}_3\text{I}$  and  $\text{GeH}_3\text{I}$  as expected since the sigma hole on  $\text{SnH}_3\text{I}$ , shown in Figure 2g, was smaller than both of those molecules.

Additionally, when furan,  $\text{CH}_3\text{OCH}_3$ , and THF were used as the Lewis bases, structures similar to those formed with  $\text{SiH}_3\text{I}$  and  $\text{GeH}_3\text{I}$  were found. These are shown in Figure 25 for furan and  $\text{CH}_3\text{OCH}_3$ . Again these were less stable than those formed with  $\text{SiH}_3\text{I}$  and  $\text{GeH}_3\text{I}$ , but their interactions were similar and the decrease in stabilization was due to the smaller sigma hole. It should be noted that in this case, pyridine no longer formed a halogen bond, as its interaction angle fell to  $48.442^\circ$ , too small to possibly form an interaction with the sigma hole. This was the result of the weakening of the sigma hole due to the center atom being changed to Sn.

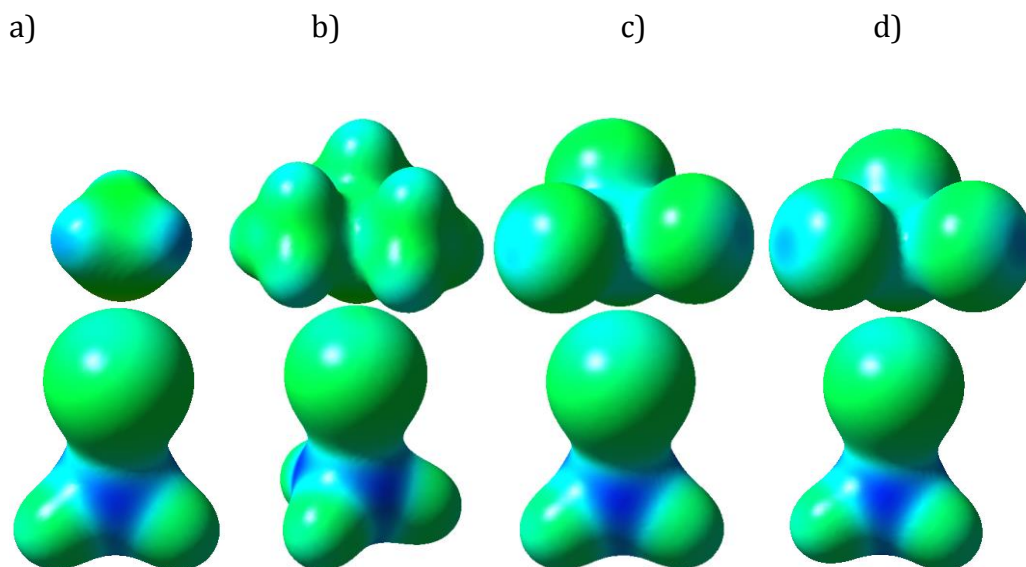


**Figure 24:** ESPs of  $\text{SnH}_3\text{I-NR}'_3$  ( $\text{R}'=\text{H, CH}_3, \text{Cl, Br}$ ): *Computed ESP map on the 0.02 iso-density surface for  $\text{SnH}_3\text{I}$  with a)  $\text{NH}_3$ , b)  $\text{N(CH}_3)_3$ ,  $\text{NCl}_3$ , and d)  $\text{NBr}_3$ . The ESPs on the surface shown were in the range  $\pm 3.09 \times 10^{-1}$  au, where areas of red were the most negative and areas of blue were the most positive.*

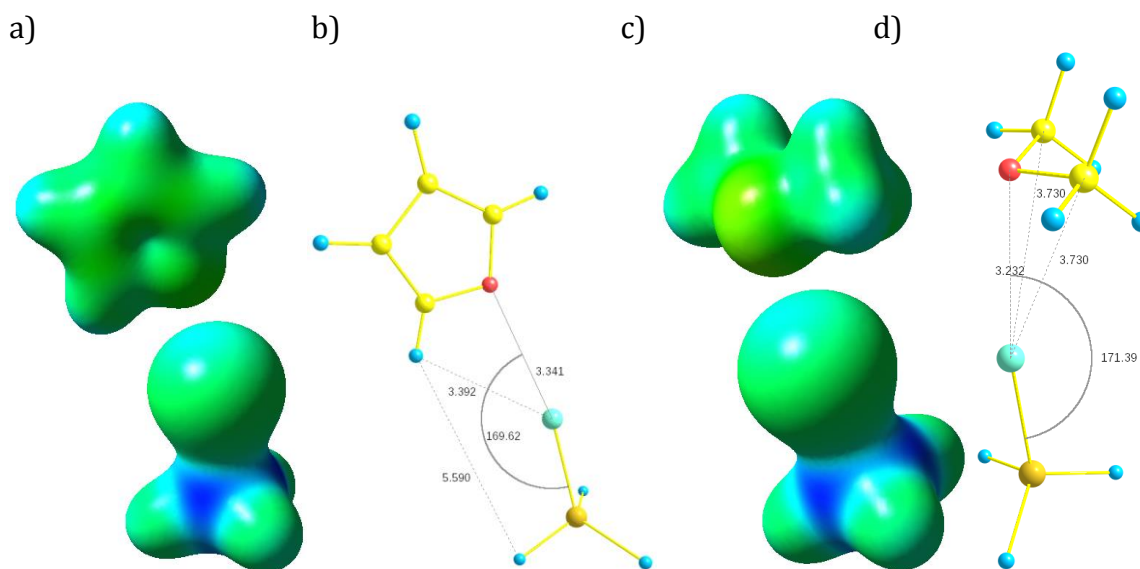


**Figure 25:** ESPs and Geometric Analysis of  $\text{SnH}_3\text{I-furan}$  and  $\text{SnH}_3\text{I-CH}_3\text{OCH}_3$ : *a,c) Computed ESP map on the 0.02 iso-density surface for  $\text{SnH}_3\text{I}$  with a) furan and c)  $\text{CH}_3\text{OCH}_3$ . The ESP on the surface shown were in the range  $\pm 3.09 \times 10^{-1}$  au, where areas of red were the most negative and areas of blue were the most positive. b,d) Geometric visualization of  $\text{SnH}_3\text{I}$  with with b) furan and d)  $\text{CH}_3\text{OCH}_3$ . These were generated and labeled in ChemCraft software.*

Unexpectedly,  $\text{H}_2\text{Se}$ , shown in Figure 26c,d formed a large bond angle of  $166.5^\circ$  that showed evidence of a halogen bond. This was the only case where a

possible halogen bond formed with that Lewis base and this analysis showed it was a weak halogen bond. The H atoms on the Lewis base were about 0.4 Å closer to the I atom than the Se atom to provide stabilization. Thus it seemed like a form of hydrogen bonding was occurring where both hydrogen atoms were interacting with the halogen along with the lone electron pair interaction with the sigma hole. Further analysis will be required outside of this thesis to determine why this stabilization occurred with this Lewis acid.

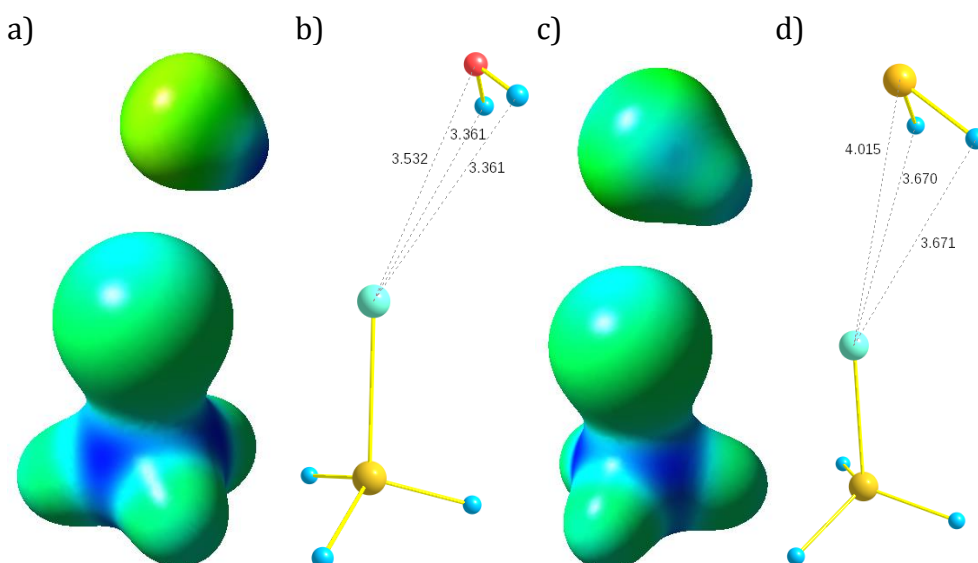


**Figure 26:** ESPs and Geometric Analysis of  $\text{SnH}_3\text{I}-\text{H}_2\text{O}$  and  $\text{SnH}_3\text{I}-\text{H}_2\text{Se}$ : *a,c)* Computed ESP map on the 0.02 iso-density surface for  $\text{SnH}_3\text{I}$  with *a)*  $\text{H}_2\text{O}$  and *c)*  $\text{H}_2\text{Se}$ . The ESP on the surface shown were in the range  $\pm 1.50 \times 10^{-1}$  au, where areas of red were the most negative and areas of blue were the most positive. *b,d)* Geometric visualization of  $\text{SnH}_3\text{I}$  with *b)*  $\text{H}_2\text{O}$  and *e)*  $\text{H}_2\text{eS}$ . These were generated and labeled in ChemCraft software.

Noting their calculated zero-point interaction energies shown in Table 4,  $\text{SnH}_3\text{I}-\text{H}_2\text{O}$  was found to be unstable after counterpoise corrections with a ZPE adjusted interaction energy of +0.13 kcal/mol.  $\text{H}_2\text{Se}$  was found to be stable with an interaction energy of -0.53 kcal/mol. Furthermore, looking at the sum of the van der Waals radii of the complexes,  $\text{H}_2\text{O}$  formed a bond distance of 3.53 Å very close to the

sum of the van der Waal radii (3.55 Å). H<sub>2</sub>Se showed stronger stabilization with a bond distance 0.13 Å shorter than the sum of the van der Waals radii, a sign of a halogen bond interaction or some other stabilizing force. Therefore H<sub>2</sub>Se formed a stronger interaction, evident by the larger bond angle, than H<sub>2</sub>O. Finally, the configurations showed the H<sub>2</sub>O molecule avoiding an eclipse with the H atoms on the Lewis base. This was not necessary with H<sub>2</sub>Se, suggesting the H atoms were being stabilized, most likely by the sides of the halogen, which had negative potential.

**3.2.8.PbH<sub>3</sub>I.** As was previously mentioned, the weakest sigma hole on MH<sub>3</sub>X (M=Si, Ge, Sn, Pb) was that of PbH<sub>3</sub>I, so the weakest halogen bonds were expected to have formed with it. However, it was able to produce bond angles of 150° or greater with the same nine Lewis bases with which the other Lewis acids formed halogen bonds as well. While this did not necessarily mean that PbH<sub>3</sub>I formed halogen bonds as successfully as the other metals, it did show that the nine Lewis bases had a high ability to halogen bond. In fact the interaction energies, shown in Table 4, with PbH<sub>3</sub>I were generally more positive than those of the other metals, which was in line with PbH<sub>3</sub>I having a smaller sigma hole.

As with the other metals, NH<sub>3</sub>, N(CH<sub>3</sub>)<sub>3</sub>, NCl<sub>3</sub>, and NBr<sub>3</sub> formed the strongest halogen bonds with bond angles of 180°. The only difference between these complexes and the complexes formed with the other metals was that the bond distances with PbH<sub>3</sub>I, shown in Table 3, were longer, a sign of the weaker interaction caused by the smaller sigma hole. The same could be said for complexes formed with NF<sub>3</sub>, pyridine, furan, THF, and CH<sub>3</sub>OCH<sub>3</sub>. With H<sub>2</sub>O shown in Figure 27,

the trend noted earlier continued and the interactions between the sigma hole and the I atom weakened, while the hydrogen bonding aspects between the I atom and H atoms increased. Thus at this point, the hydrogen atoms, and not the lone pairs on the O atom were stabilizing the complex. This was supported further from the interaction energy values, shown in Table 4. Where as before the interaction energies with H<sub>2</sub>O were all positive, with PbH<sub>3</sub>I the interaction energy was negative at -0.10 kcal/mol.

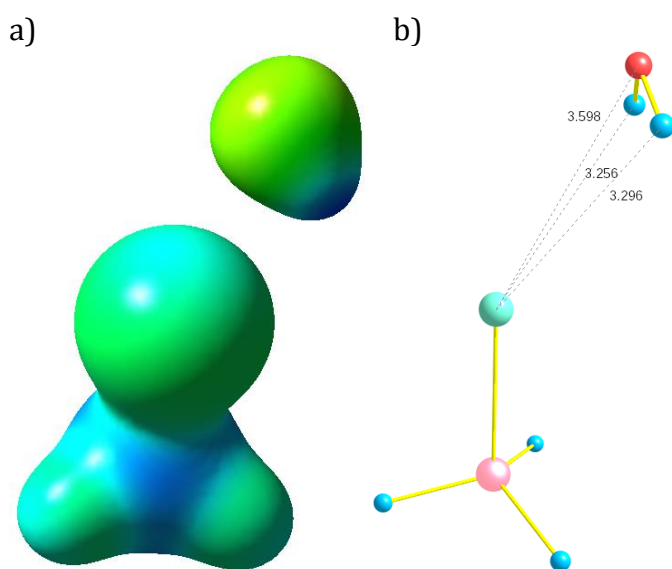


**Figure 27:** ESP and Geometric Analysis of PbH<sub>3</sub>I-H<sub>2</sub>O: a) Computed ESP map on the 0.02 iso-density surface for PbH<sub>3</sub>I with H<sub>2</sub>O. The ESPs on the surface shown were in the range  $\pm 3.09 \times 10^{-1}$  au, where areas of red were the most negative and areas of blue were the most positive. b) Geometric visualization of PbH<sub>3</sub>I with H<sub>2</sub>O. This was generated and labeled in ChemCraft software.

**3.2.9. Halogen Bonding Analysis Conclusions.** The trends observed by Donald et al.<sup>10,11</sup> have been shown to be consistent with the molecules tested in this work. Halogen bonding interactions increased in stability going from X = F to X = I. Additionally, using Si as the center atom for the Lewis acid resulted in the more

stable complexes than Ge, Sn, and Pb, with Pb producing the least stable. In general,  $\text{NF}_3$ ,  $\text{NCl}_3$ , furan,  $\text{H}_2\text{O}$ ,  $\text{NBr}_3$ ,  $\text{N}(\text{CH}_3)_3$ ,  $\text{CH}_3\text{OCH}_3$ ,  $\text{NH}_3$ , and THF showed the most affinity for halogen bonding, although  $\text{NF}_3$ ,  $\text{NH}_3$ , and  $\text{H}_2\text{O}$  required the larger sigma holes.

**3.3. Failure to Halogen Bond.** Unlike Tawfik and Donald's work, there were many cases where the interaction angles of the molecules were so small that it was not necessary to analyze them to confirm that no halogen bonding had occurred. Generally, most Lewis bases either always halogen bonded or never did, with  $\text{H}_2\text{O}$ ,  $\text{H}_2\text{S}$ , and  $\text{H}_2\text{Se}$  being the exceptions.

**3.3.1.  $\text{H}_2\text{O}$ ,  $\text{H}_2\text{S}$ , and  $\text{H}_2\text{Se}$ .** These Lewis bases were still able to form large angles of interaction with the Lewis acids. It has already been shown in Section 3.2. that these Lewis bases fell near the  $150^\circ$  cutoff angle that was utilized in this work. With some of those cases, the lone electron pairs on the Lewis bases did not face directly at the sigma hole on the Lewis acids, so they were determined not to be forming halogen bonds. Since they were addressed in that section, they will not be addressed again here.

In the cases where the angle of interaction was well below the  $150^\circ$  cutoff angle, it was clear that the interactions were of hydrogen bonding nature. Figure 28 shows an example of how these Lewis bases interact at smaller angles with the Lewis acid. This shows the hydrogen bonding exhibited by the Lewis bases. The one H atom was closest to the negative potential on the I atom (not the sigma hole), while the Se atom was closer to a H atom on  $\text{GeH}_3\text{I}$ , which had positive potential.

According to the interaction energies, shown in Table 4, this interaction was very stable and was what the complexes preferred rather than halogen bonding.

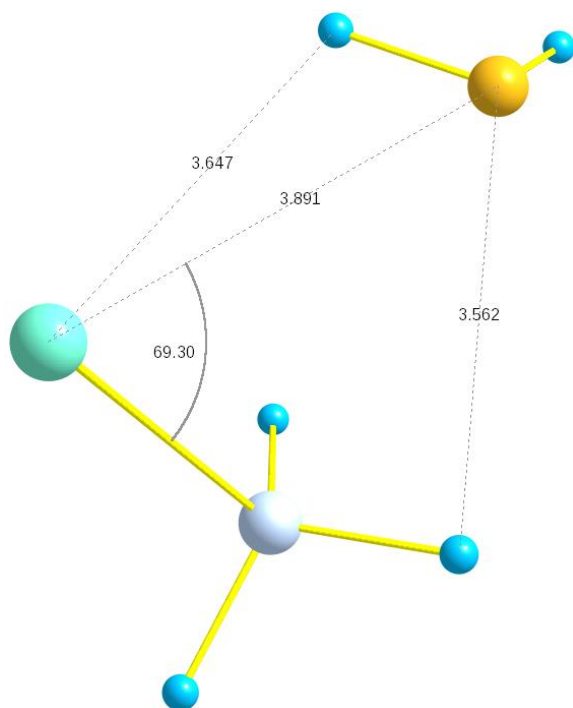


**Figure 28:** Geometric Analysis of  $\text{GeH}_3\text{I}-\text{H}_2\text{Se}$ : Geometric visualization of  $\text{GeH}_3\text{I}$  with  $\text{H}_2\text{Se}$ . This was generated and labeled in ChemCraft software.

**3.3.2. Pentafluoropyridine.** There were no cases where F-py was able to halogen bond. The cause of this was obvious, the F atoms. Halogen bonding requires an electron rich Lewis base, and an electron deficient sigma hole. The F atoms on F-py pulled the electron density away from the N atom, which was where the halogen bond interaction occurred. Because of this, only a strong sigma hole could form halogen bonds with this Lewis base. Tawfik and Donald<sup>11</sup> found it possible to form halogen bonds with their larger sigma holes, but it seemed that the smaller sigma hole caused by the H atoms on  $\text{MH}_3\text{X}$  were not capable of supporting such interactions.



Rather than halogen bond, they stabilized to complexes of the form shown below in Figure 29. Geometric configuration made it clear that the original linear geometry the complexes started out with had changed drastically. The molecule moved entirely so that the  $\text{SnH}_3\text{I}$  lined itself up with the ring of the F-py. Unfortunately the interactions were so weak with this molecule that in some cases, computational limitations prevented an energy minimum from being computed before this work was submitted. It was expected that the molecules would continue to move until the I atom was located towards the center of the ring system, away from the F atoms. The final configurations of systems like this will be discussed in future work.

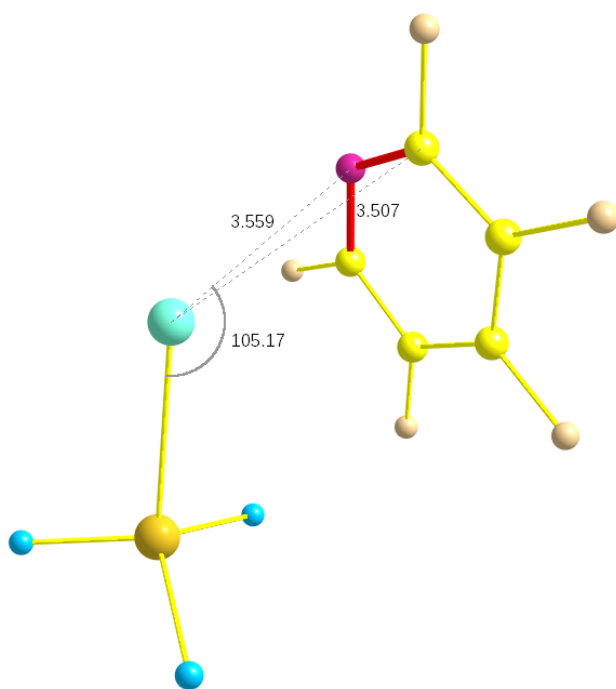


**Figure 29:** Geometric Analysis of  $\text{SnH}_3\text{I}$ -(F-py): *Geometric visualization of  $\text{SnH}_3\text{I}$  with with F-py. This was generated and labeled in ChemCraft software.*

#### 4. Summary and Outlook

It has been shown that halogen bonding is possible with molecules of the form  $MH_3X$  ( $M = C, Si, Ge, Sn, Pb$ ;  $X = Cl, Br, I$ ). These interactions were much weaker than halogen bonds formed with  $MF_3X$  ( $M = C, Si, Ge, Sn, Pb$ ;  $X = Cl, Br, I$ ), previously studied by Tawfik and Donald.<sup>11</sup> This result was expected since the lack of F atoms on the Lewis acid resulted with a smaller and weaker sigma hole, a key component of halogen bonding. With molecules that did halogen bond, trends found previously were consistent with these different Lewis acids.

The first trend that was noted was that going from F to I down the periodic table for the halogen when the halogen donor was  $CH_3X$  caused an increase in the stability of the halogen bonds. Additionally moving down the periodic table for the center atom on the halogen donor  $MH_3I$  caused a decrease in the stability of the halogen bonds. Finally, the inability of  $CH_3F$  to halogen bond might have been expected given the well known difficulties associated with inducing a sigma hole on F, or donating any electron density from a F atom in a bond. These three trends were consistent with those seen previously by Donald et al.<sup>10,11</sup>

A deviation from previous work was found with the molecules that did not halogen bond or some of the exceptions found. As opposed to previous work by Tawfik and Donald<sup>11</sup>, this study found that many complexes could not form halogen bonds. Additionally, in some cases halogen bond configurations were found but the interaction energies were repulsive. This, again, was expected since this work focused on the use of smaller sigma holes. Of note was the fact that  $H_2O$ ,  $H_2S$ , and

H<sub>2</sub>Se could not halogen bond in most cases. This indicated that molecules of that or similar form require a larger sigma hole.

Overall it was found that halogen bonding interactions could exist with these molecules, but usually they were weak and relied on other interactions to fully stabilize the complexes. It is hoped that this work will help provide more information about the uses and possibilities of halogen bonding. There is also more work to be done with some of the information collected for this project. There were some molecules that did not fully optimize by the time of this report, so it is hoped that in the future it can be revisited. Additionally, work has been done to study P based Lewis bases and their halogen bonding abilities that was not mentioned in this work, but will be addressed in the future.

## **5. Acknowledgements**

This work was supported by Summer Research Fellowships from the National Science Foundation (through a NSF CAREER award to Dr. Kelling Donald CHE-1056430) and a Pierce Award from the University of Richmond, School of Arts and Sciences. Dr. Donald at the University of Richmond served as the primary advisor on the project. Dr. Donald along with Dr. René Kanters, also at the University of Richmond, served as the honors thesis readers for this work. The University of Richmond and the MERCURY consortium provided computational resources.

## 6. References

- (1) Legon, A. C. The Halogen Bond: an Interim Perspective. *Phys. Chem. Chem. Phys.* **2010**, *12*, 7736-7747.
- (2) F. Gunthrie, *J. Chem. Soc.*, **1863**, *16*, 239.
- (3) H. A. Benesei and J. H. Hildebrand, *J. Am. Chem. Soc.*, **1949**, *71*, 2703.
- (4) O. Hassel and C. Romming, *Q. Rev. Chem. Soc.*, **1962**, *16*, 1.
- (5) O. Hassel, *Science*, **1970**, *170*, 497.
- (6) R. S. Mulliken and W. B. Person, *Molecular complexes: a lecture and reprint volume*, Wiley-Interscience, New York, **1969**.
- (7) H. A. Bent, *Chem Rev.*, **1968**, *68*, 587-648.
- (8) Wang, C.; Danovich, D.; Mo, Y.; Shaik, S. On the Nature of the Halogen Bond. *J. Chem. Theory Comput.* **2014**, *10*, 3726-3737.
- (9) Clark, T.; Hennemann, M.; Murray J. S.; Politzer, P. Halogen bonding: the  $\sigma$ -hole (Proceedings of "Modeling interactions in biomolecules II", Prague, September 5th-9th, 2015). *J. Mol. Model.* **2007**, *13*, 291-296.
- (10) Donald, K.; Wittmaack, B. K.; Crigger, C. Tuning Sigma-Holes: Charge Redistribution in the Heavy (Group 14) Analogues of Simple and Mixed Halomethanes can Impose Strong Propensities for Halogen Bonding. *J. Phys. Chem.* **2010**, *114*, 7213-7222.
- (11) Tawfik, M; Donald, K. J. Halogen Bonding: Unifying Perspective on Organic and Inorganic Cases. *J. Phys. Chem. A.*, **2014**, *118*, 10090-10100.
- (12) Politzer, P.; Murray, J. S. Halogen Bonding: an Interim Discussion. *ChemPhysChem* **2013**, *14*, 278-294.

- (13) De Moliner, E.; Brown, N. R.; Johnson, L. N. Alternative Binding Modes of an Inhibitor to two Different Kinases. *Eur. J. Biochem.* **2003**, *270*, 3174-3181.
- (14) Auffinger, P.; Hays, F. A.; Westhof, E.; Shing-Ho, P. Halogen Bonds in Biological Molecules. *Proc. Natl. Acad. Sci. U.S.A.* **2004**, *101*, 16789-16794.
- (15) Metrangolo, P.; Neukirch, H.; Pilati, T.; Resnati, G. Halogen Bonding Based Recognition Processes: A World Parallel to Hydrogen Bonding. *Acc. Chem. Res.* **2005**, *38*, 386-395.
- (16) The ChemCraft graphical program: <http://www.chemcraftprog.com>.
- (17) Head-Gordon, M.; Head-Gordon, T. Analytic MP2 frequencies without Fifth-Order Storage. Theory and Application to Bifurcated Hydrogen Bonds in the Water Hexamer. *Chem. Phys. Lett.* **1994**, *220*, 122-128 and references therein.
- (18) Frisch, M. J.; Trucks, G. W.; Schlegel, H. B.; Scuseria, G. E.; Robb, M. A.; Cheeseman, J. R.; Scalmani, G.; Barone, V.; Mennucci, B.; Petersson, G. A.; et al. *Gaussian 09*, revision A.1; Gaussian, Inc.: Wallingford, CT, **2009**.
- (19) The Stuttgart/Cologne correlation consistent triple-zeta (cc-pVTZpp) basis sets used are from the website: <http://www.tc.uni-koeln.de/PP/clickpse.en.html>.
- (20) Peterson, K. A. Systematically Convergent Basis Sets with Relativistic Pseudopotentials. I. Correlation Consistent Basis Sets for the Post-d Group 13-15 Elements. *J. Chem. Phys.* **2003**, *119*, 11099-11112 (for Sn and Pb).
- (21) Peterson, K. A.; Shepler, B. C.; Figgen, D.; Stoll, H. On the Spectroscopic and Thermochemical Properties of ClO, BrO, IO, and Their Anions. *J.*

*Phys. Chem. A.* **2006**, *110*, 13877-13883 (for I).

(22) For description of this procedure, see: Jensen, F. *Introduction to Computational Chemistry*; Wiley: New York, **199**; pp 172-173.